UNIVERSIDADE DE LISBOA
FACULDADE DE CIÊNCIAS
DEPARTAMENTO DE QUÍMICA E BIOQUÍMICA

Cyclodextrins as anti-asthmatic drug carriers: an *in silico* study

Bruno Emanuel de Sá Calçada

Dissertação
Mestrado em Química
Química

2014

UNIVERSIDADE DE LISBOA
FACULDADE DE CIÊNCIAS
DEPARTAMENTO DE QUÍMICA E BIOQUÍMICA

Cyclodextrins as anti-asthmatic drug carriers: an *in silico* study

Bruno Emanuel de Sá Calçada

Dissertação
Mestrado em Química
Química

Tese orientada por Doutor Miguel Machuqueiro e Professora Doutora Helena Cabral Marques

2014

Abstract

Asthma is a chronic disease that affect millions of persons around the world and it has gained an increasing concern in the world health organizations. To fight this disease there are some options, the short acting β-2 agonist salbutamol, or the inhaled corticosteroids, like beclomethasone dipropionate, budesonide, ciclesonide and fluticasone propionate.

Cyclodextrins are a family of oligosaccharides containing several D-glucopyranose units linked by α(1-4) glycosidic bonds. The three most common used, α-, β- and γ-cyclodextrins, and some of their derivatives are widely used in the pharmaceutical industry as excipients with the main purpose of complexing with the anti-asthmatic drugs and increase their aqueous solubility, stability and bioavailability.

In this work, using molecular docking and quantum mechanics calculations, it was possible to identify the preferential binding modes and calculate their energies of binding. The space inside the cyclodextrins' cavities is important for the accommodation of guest molecules, influencing the degree of inclusion. α- and γ-cyclodextrins are not very good hosts because their cavity spaces are too small or too large, respectively. On the other hand, β-cyclodextrin and its derivatives (methyl- and 2-hydroxypropyl-cyclodextrins) exhibited very good size complementary with the drugs studied. 2-hydroxypropyl-β-cyclodextrin appeared to be particularly good forming stable adducts with most drugs. This cyclodextrin seems to conjugate the correct cavity size, with increased hydrophobicity and extra hydroxyl groups for non-specific and specific interactions with the guests, respec-

tively.

In overall, our computational approach was able to correctly predict qualitatively the best matches between the anti-asthmatic drugs and the cyclodextrins. An example is the adduct formed between salbutamol and 2-hydroxypropyl-β-cyclodextrin, with no stability values measured experimentally, which we expect to be very strong. This remarkable predictive ability shows that our computational method can be a powerful tool designing new and unexplored combinations of adducts.

Keywords: asthma, adducts, free energy, molecular docking, quantum mechanics

Resumo

A asma é uma doença crónica que afeta milhões de pessoas em todo o mundo e tem vindo a aumentar o seu número de casos nas últimas décadas. Atualmente a Organização Mundial de Saúde considera-a uma das principais doenças. O combate à asma iniciou-se em 1960 com a descoberta dos recetores adrenérgicos e subsequente, o recetor β. Com esta descoberta desenvolveram-se os agonistas β-2 de ação curta como o salbutamol, específicos para o recetor β-2, mais tarde na década de 80 surgiram os agonistas β-2 de ação prolongada. Foi no início da década seguinte que se descobriram os corticosteróides, como a beclometasona dipropionato, budesonida, ciclesonida e fluticasona propionato, muito importantes no tratamento de casos mais severos de asma.

As ciclodextrinas são oligossacáridos cíclicos, constituídos por várias unidades de D-glucopiranose conectadas através de uma ligação glicosídica α(1-4). Atualmente existem três ciclodextrinas principais, que são: a α, a β e a γ. A descoberta das ciclodextrinas remonta ao final do século XIX quando foram extraídas pela primeira vez. Desde então muitos grupos de investigação dedicaram-se à síntese e caraterização destes compostos. As suas propriedades físico-químicas foram o que levaram ao desenvolvimento dos seus derivados de modo a melhorar as propriedades das anteriores. Nos dias de hoje têm uma ampla aplicação, desde a indústria alimentar, à cosmética e farmacêutica. A sua importância ao nível da indústria farmacêutica prende-se com o facto das ciclodextrinas melhorarem a solubilidade, estabilidade e biodisponilidade dos fármacos.

Para estudar os modos de ligação e energias livres dos complexos formados entre ciclodextrinas e fármacos, foram selecionadas cinco ciclodextrinas, as três mais comuns, α, β e γ-ciclodextrinas, e duas derivadas da β-ciclodextrina, a metil- e 2-hidroxipropil-β-ciclodextrinas. Os fármacos seleccionados foram o salbutamol, agonista β-2 de ação curta, atualmente o mais utilizado no mercado e quatro corticosteróides de resposta prolongada, a beclometasona dipropionato, budesonida, fluticasona propionato e o pro-fármaco ciclesonida.

Inicialmente, neste estudo, otimizaram-se as estruturas das moléculas com o programa Avogadro, usando o método de "steepest descent" e o campo de força MMFF94. De seguida, as otimizações de geometria foram realizadas ao nível quântico com o Gaussian 09, com funcional PBE1PBE e a basis set 6-31G(d,p). Todos os cálculos foram realizados em vácuo com carga zero e multiplicidade um. Foram também calculadas as frequências destes compostos de modo a garantir que a estrutura otimizada é um mínimo de energia. Após estes cálculos iniciais, deu-se início a um estudo de docking molecular. Recorrendo ao programa AutoDockTools foram preparados os ficheiros de iniciação com a remoção dos átomos não polares em todas as estruturas e introdução de flexibilidade nos fármacos. De seguida foi preparada uma grelha centrada no recetor, neste estudo são as ciclodextrinas, com largura suficiente na região superior e inferior de modo a serem explorados os modos de ligação com o programa AutoDock Vina. De cada estudo resultaram aproximadamente mil soluções que de seguida sofreram um processo de permutação, devido à elevada simetria dos recetores, que podiam dar a ilusão de termos soluções muito diferentes quando na realidade apenas estão em subunidades diferentes. Estas estruturas também foram agrupadas em clusters de modo a facilitar o estudo dos modos de ligação preferenciais. A partir do docking molecular vários modos de ligação foram selecionados. O critério para seleção destes modos de ligação foram: o tamanho do cluster, isto é, o número de soluções que o compõem, e as energias do docking. Para cada cluster selecionado apenas é estudada a estrutura com a menor energia. Entramos agora na ùltima fase do

nosso estudo, com a seleção de dois a quatro modos de ligação para cada complexo. Procedemos mais uma vez ao cálculo das estruturas otimizadas usando mecânica quântica e parâmetros iguais aos utilizados no início deste estudo. O objetivo passou por obter a estrutura otimizada de cada modo de ligação, mas também garantir que a estrutura é um mínimo de energia, bem como calcular as respetivas energias livres através de cálculos de frequências.

A partir dos resultados de docking molecular e posterior otimização de geometria é possível dizer que a α-ciclodextrina, para estes casos, não aparenta ser um bom composto de inclusão na medida que apenas introduz na sua cavidade uma cadeia lateral dos fármacos maiores e mesmo no caso do fármaco mais pequeno a estrutura mais estável é a de não inclusão. No caso da β-ciclodextrina existe uma maior variedade de modos de ligação e um aumento no nível de inclusão dos fármacos. A metil-β-ciclodextrina com a substituição do átomo de hidrogénio por um grupo metilo na região mais larga das ciclodextrina onde existiam dois grupos hidroxilo por subunidade, verificou-se uma dificuldade por parte dos fármacos em interagir neste lado, levando assim a uma diminuição na propriedade deste recetor em atuar como doador de ligações de hidrogénio. Neste caso, o aumento da hidrofobicidade que podendo ter um papel importante na afinidade, veio diminuir a especifidade do recetor para estes ligandos. No caso da 2-hidroxipropil-β-ciclodextrina, com a substituição do átomo de hidrogénio no grupo hidroxilo primário na zona mais estreita da ciclodextrina por um grupo 2-hidroxipropilo, observamos um aumento da hidrofobicidade da cavidade enquanto também aumentou a possibilidade de criar ligações de hidrogénio com o grupo adicionado. Com esta alteração o nível de inserção dos fármacos, principalmente dos corticosteróides aumentou, provavelmente devido a uma melhorar acomodação no interior da cavidade, mas também devido à possibilidade de criação de ligações de hidrogénio em ambos os lados das ciclodextrina.

No que toca às energias de ligação, grande parte ainda se encontra a calcular, à exceção dos complexos com o salbutamol. Os resultados estão de acordo

com os obtidos no docking molecular, sendo que a α- e γ-ciclodextrinas obtiveram os piores valores devido às suas cavidades serem demasiado pequenas ou grandes, respetivamente. As baixas energias de ligação para a β- e metil-β-ciclodextrinas estão em excelente concordância com os maiores valores da constante de estabilidade medidos experimentalmente. Curiosamente, os nossos dados computacionais indicam que o salbutamol teria uma constante de solubilidade maior caso a 2-hidroxipropil-β-ciclodextrina fosse utilizada como recetor.

Em conclusão, a nossa abordagem computacional foi capaz de prever qualitativamente as melhores complementaridades entre os fámacos anti-asmáticos e as ciclodextrinas. Esperamos que as energias livres de ligação de Gibbs, quando terminadas, corroborem o que já foi observado. Um exemplo, é o complexo formado entre o salbutamol e a 2-hidroxipropilo-β-ciclodextrina, cuja constante de estabilidade não foi estudada experimentalmente, mas esperamos que seja elevada.

Esta notável capacidade preditiva mostra que o nosso método computacional pode ser uma ferramenta poderosa na conceção de novas e inexploradas combinações de complexos.

Palavras-chave: asma, complexos, energia livre, docking molecular, mecânica quântica

Acknowledgments

My acknowledgment to Professor Helena Marques for accepting me in her research group, for showing me how useful cyclodextrins can be and for always being available to help. A special thank you to Professor Maria Frazão for introducing us.

My acknowlegment to Miguel Machuqueiro for taking me under his wing, for helping me during this year, for the patience with all my question, for...everything. You have my gratitude Professor ☺.

To my officemates, Diogo Vila-Viçosa for all the help, since the clarification of my doubts to the help with the scripts, and to Rafael Nunes for the awesome chocolates that he brought in the last months and also for the brainstorming of crazy and not so crazy ideas during this last year.

My acknowledgment to Vitor Teixeira, for showing me the wonders of AutoDock programmes, how helpful they can be and also for the patience everytime i was showing him some results on AutoDockTools or PyMOL.

My acknowledgment to Professor Maria José Calhorda for accepting in the inorganic and theoretical chemistry group.

In a more personal level, to my parents and brother, to my family and friends, and to Marisa, for all the support and patience. Thank you for the interest in what i was doing even when you didn't understand quite well what it is.

For last but not least, to the ones lost but not forgotten.

Contents

List of Figures

List of Tables

List of Abbreviations

SAL	salbutamol
BDP	beclomethasone dipropionate
FP	fluticasone propionate
BUD	budesonide
CIC	ciclesonide
CyDs	cyclodextrins
α-CyD	alpha-cyclodextrin
β-CyD	beta-cyclodextrin
γ-CyD	gamma-cyclodextrin
CGTase	Cyclodextrin Glycosyl Transferase
Me-β	methyl-β
Hp-β	2-hydroxypropyl-β
K_s	stability constant
QM	quantum mechanics
SCF	self-consisting field
MM	molecular mechanics
HF	Hartree-Fock
DFT	density functional theory
RMSD	root mean square deviation
ΔE	electronic binding energies
ΔH	enthalpic binding energies
ΔG	Gibbs binding energies

Chapter 1

Introduction

1.1 Asthma

Asthma is a chronic disease whose history is characterized by recurring episodes of lack of air. Its definition contains four components: symptoms and variable airflow obstruction (bronchoconstriction), easily assessed by clinicians; airway inflammation and airway hyper-responsiveness, that are less accessible to the clinical practice and characterise the subjacent disease. Despite all this four domains being usually present, the diagnose of asthma is mainly based on the symptoms associated with the narrowing of small airways and possibly include shortness of breath, wheezing, chest tightness and cough. However this symptoms are not specific and exclusive to this disease and can be found in other respiratory conditions like, chronic obstructive pulmonary disease and even in nonrespiratory diseases such as obesity and cardiac failure [**1, 2**].

Asthma is a disease recognized since the ancient times [**3**], nowadays is considered an inflammatory disorder with an high level of prevalence, affecting 300 million people worldwide and is expected to affect 100 million more until 2025 [**4**]. In addiction to its effect on people, asthma is also associated

with an enormous economic burden on health care systems and society. **[5]**.

The Global Initiate for Asthma (GINA) guidelines provided a schema to classify asthma severity into four steps, regarding the clinical features of patients before treatment and the response to the treatment according to the daily medication **[6]**. Despite all the advances in understanding this disease and a growing acceptance of these guidelines, an inadequate control of asthma is still common, with nefarious consequences to various aspects of daily life, including sleep, work, study and exercise **[4]**.

1.2 Anti-asthmatic drugs

For centuries, strong coffee and tea were recommended for the relief of asthma, then in the beginning of the 20^{th} century epinephrine (or adrenaline), became the standard bronchodilator used for the treatment of asthma. But in the 60s decade, a breakthrough happened with the discovery of the adrenergic receptors, divided into the α and β receptors, with a subdivision into the β-1, located in the heart and intestinal smooth muscle, and the β-2 on the bronchial and uterus smooth muscle. With this discovery, the β-agonists emerged, first was isoprenaline and, later on, salbutamol (SAL) (**Figure 1.1e**) was developed as a selective β-2 agonist; becoming nowadays the most used short acting β-2 agonist in the treatment of asthma. The last step in this discovery series came in the 1980s with the development of the long acting β-2 agonists, like salmeterol and formoterol, with fast acting mechanisms and prolonged effects ($>$ 12 hours) **[3]**.

During the next decade a new type of drugs, that were already in development but not yet in the market due to some side effects and its poor lung selectivity by the inhaled route, reached a turning point with the discovery of beclomethasone dipropionate (BDP), an inhaled corticosteroid. Since then, others corticosteroids were developed, like fluticasone propionate (FP), budesonide (BUD), and a few years ago in 2008, ciclesonide (CIC), a pro-drug that is transformed in its active form by the esterases in

the lungs (**Figures 1.1a-d**) [1].

Presently, these two approaches for the treatment of asthma are the most used, individually or combined, depending on the severity of the asthma case. However, there are other treatments like anti-leukotrienes and anti-immunoglobulin E.

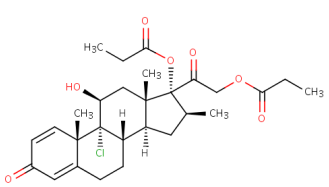

(a) Beclomethasone dipropionate (BDP)

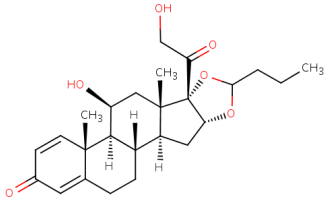

(b) Budesonide (BUD)

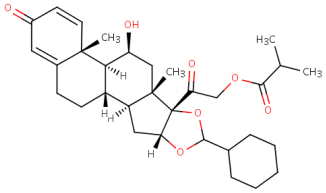

(c) Ciclesonide (CIC)

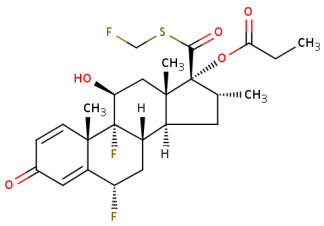

(d) Fluticasone propionate (FP)

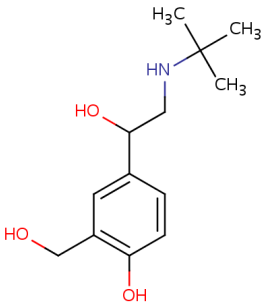

(e) Salbutamol (SAL)

Figure 1.1: Schematic structure of the anti-asthmatic drugs used in this study.

1.3 Cyclodextrins

The cyclodextrins (CyDs) are cyclic oligosaccharides of several D-glucopyranose units linked by α(1-4) glycosidic bonds. There are 3 native and most

commonly used CyDs: α-cyclodextrin (α-CyD), β-cyclodextrin (β-CyD) and γ-cyclodextrin (γ-CyD), consisting of six, seven and eight units, respectively [**7**].

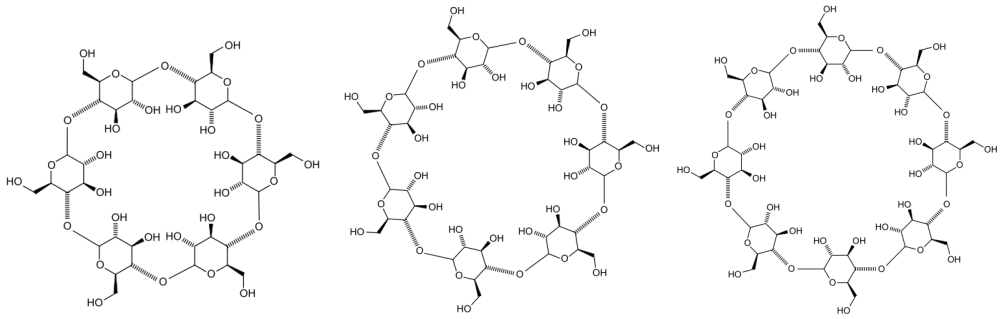

(a) α-CyD **(b)** β-CyD **(c)** γ-CyD

Figure 1.2: Schematic structures of α-, β- and γ-cyclodextrins. Image adapted from [8] .

1.3.1 A scope through history

The first reference of a substance that later was shown to be a CyD occurred in 1891 [**9**]. Villiers, a french scientist obtained a small amount of a crystalline product, that he called *"cellulosine"*, by digesting starch, one of the most abundant carbohydrates in nature as cellulose and sucrose, with *Bacillus amylobacter*. Many scientists later on, defended that he used impure cultures and the cyclodextrins were indeed produced by another bacteria, *Bacillus macerans*. This bacteria provided the cyclodextrin glycosyl transferase (CGTase, EC 2.4.1.19) the enzyme responsible for the production of the cyclic dextrin or cyclodextrin, which included the most common ones, but also some large cyclodextrins with more than nine units of glucopyranose [**10**–**12**].

During the 20^{th}, century there were many research groups involved in the production of cyclodextrins. Many authors divide this century in three major stages of development for the CyDs technology [**9**]:

- The discovery period - It started with Villiers' discovery and ended in the late 30s. It was a time marked by the findings of Franz Schardinger, an Austrian microbiologist, that isolated two different dextrins which he called α- and β-dextrin using the starch and the microorganism *Bacillus macerans*, and for the elucidation of the cyclic structure of these two dextrins, by Freudenberg and his coworkers in the second half of 1930s [**13**].

- The exploration period - From 1936 until 1970, it was a time of high level research and discovery. Between 1948-50 γ-CyD was discovered and its structure was elucidated. In the beginning of 1950, French and Cramer groups began to work on the enzymatic production of CyDs with the main goal to isolate them with high level of purity and characterise their real physicochemical properties. Cramer and coworkers obtained in 1953 the first patent regarding this subject covering the most important aspects of the CyDs applications. The first review was published by French in 1957 along with the first misinformation concerning the toxicity of cyclodextrins. Until this date not much had been published about toxicological studies of CyDs, discouraging many scientists to develop products containing CyDs for two and half decades. By the end of 1960s, the methods to prepare cyclodextrins on a laboratory scale, their structure and physicochemical properties were elucidated [**9, 11, 13**].

- The industrial period - Many industries got involved in the production of CyDs and a product that a while ago costed two thousand dollars per kilogram, and was only available as a rare chemical, started to be produced by half a dozen of industries worldwide and the price lowered to near five dollars. Not only the quantity produced increased but also its quality during production, due to improvements in the genetic engineering with the design of different types of CGTases, more active and specific than the previous ones [**9, 11, 13**].

1.3.2 Physicochemical properties

The most important structural feature that is evidenced from the three-dimensional structures of CyDs is their torus shape with secondary hydroxyl groups located in the wider edge of the ring, whereas the primary hydroxyl groups are in the narrow edge. This structure provides the CyD an hydrophilic outside with the ability of dissolve in water and an hydrophobic cavity allowing them to form stable complexes with guest molecules [**9, 10**].

In the next table (**Table 1.1**) there are presented some physicochemical properties of the most common cyclodextrins and two derivatives of β-CyD, methyl-β- (Me-β-) and 2-hydroxypropyl-β-CyD (Hp-β-CyD).

Table 1.1: Properties of the cyclodextrins used in this work.

Properties	Cyclodextrins				
	α	β	Me-β	Hp-β	γ
no. of subunits	6		7		8
formula	$C_{36}H_{60}O_{30}$	$C_{42}H_{70}O_{35}$	$C_{49}H_{84}O_{35}$	$C_{63}H_{112}O_{42}$	$C_{48}H_{80}O_{40}$
MW, Da	972.85	1134.99	1312	1400	1297.14
cavity diam., Å	4.7-5.3		6.0-6.5		7.5-8.3
solubility [a]	145	18.5	>500	>600	232

[a] Solubility in pure water at about 25°C ($mg \cdot ml^{-1}$)[**11**].

The surrounding water molecules can have an important role in the aggregation process of cyclodextrins, which results in the different solubilities observed. In fact, an odd number of subunits enhances the probability of making intramolecular hydrogen bonds, increasing aggregation and lowering solubility [**7**]. The structural modifications of the parental cyclodextrins led to new derivatives with improved properties and new applications.

The driving forces leading to the inclusion properties of CyDs include: dipole-dipole electrostatic interactions; the van der Waals interactions, in specific, the dipole-induced dipole interactions and the London dispersion forces; hydrophobic interactions; and hydrogen bonding [**14**].

1.3.3 Drug delivery systems

Drugs require good water solubility and, at the same time, lipophilicity enough to cross the membrane. Therefore one of the most important properties, for cyclodextrins to be considered an excellent carrier, is their solubility. CyDs have the ability to incorporate drugs and increase their delivery in the biological membranes, increasing the availability near the membrane and in the bloodstream [**15**].

Another important aspect of the encapsulation is the improved stability of the drugs, making them less vulnerable to degradation due to chemical reactions, heat or light. This inclusion is also important when dealing with drugs that cause irritation, for instance, of the gastric mucosa when administrated orally [**10**].

CyDs are mostly biologically inactive, since they are poorly absorbed in the membrane, probably due to the bulky shape and hydrophilic nature. Their lack of toxicity are also relevant for industries that want to use cyclodextrins as excipients in the formulation of drugs [**15**].

1.3.4 Cyclodextrins adducts with anti-asthmatic drugs

There are already experimental data measured for the association between these cyclodextrins and anti-asthmatic drugs. In **Table 1.2** are presented the stability constants (K_s) available in the literature. K_s measures the strength of the interaction between two molecules (guest and host) that come together to form the adduct. Higher values of the constant corresponds to more stable adducts. The SAL drug forms very stable complexes with β-CyD and its derivative, Me-β. BDP clearly prefers the Hp-β-CyD, while BUD and FP have their higher stability when complexed with the larger γ-CyD. CIC forms a very stable adduct with Me-β-CyD. The general trend from the data in **Table 1.2** is that these drugs prefer to interact with

larger CyDs, and in some cases, also prefer some derivatives instead of the unmodified CyDs.

Table 1.2: Stability constants values (M^{-1}) for the available adducts at different temperatures.

Drugs	Temperature / °C	CyDs					Reference
		α	β	Me-β	Hp-β	γ	
BDP	25	226.7	22.6		681.6		[**16**]
BUD	-				1195	4578	[**17**]
CIC	25			14880			[**18**]
	-				743.7	149.7	[**19**]
FP	-				192.9	3093.7	[**20**]
SAL	37	1.3	68.9	82.7		5.2	[**21**]
	25	1.1	69.3	61.9		5.1	
	20	1.1	66.4	78.7		5.1	

1.4 Quantum and Molecular Mechanics

At the end of the 19^{th} century, classical mechanics was the most used tool to predict the dynamic movement of *material bodies*, based on Maxwell's electromagnetism theory. But with the beginning of 20^{th}, the theories, so far believed to explain the physical phenomena, were challenged by Einstein's theory of relativity and by the new experimental techniques developed at a microscopic level [**22**].

With the failure of classical physics to explain some phenomena such as black-body radiation, atomic stability and atomic spectroscopy, a first breakthrough came with the discovery of Max Planck introducing the concept of the quantum of energy, triggering an increase in the discoveries and a all new way of thinking. Based on Planck's quantum concept discovery, Einstein was able to introduce the photon concept and explain the photoelectric problem. Bohr, after the discoveries of Rutherford (atomic nucleus), Planck (quantum concept) and Einstein (photons), introduced the hydrogen atom model where emission or absorption of radiation by atoms occurs in tran-

sitions at various discrete energy states. Them Compton in 1923 gave the conclusive confirmation of the corpuscular nature of light by scattering X-rays with electrons [**23**].

These researchers postulates and ideas were in agreement with experimental results but lack in the basis of a consistent theory, led Heisenberg and Schrödinger to the search for the theoretical foundation underlying the ideas developed in the last 25 years and to the principles of nowadays old quantum mechanics (QM).

The main objective of QM is to determine the spatial positions of all the nucleus and electrons of the system in study. The electrons of the molecules are allowed to move in the field of a fixed nuclei, applying the Born-Oppenheimer approximation, until they reach a self-consisting field (SCF) [**24**]. At this moment the attractive and repulsive forces of all the electrons in the system and the fixed nuclei are in a stationary state. The nuclei are moved, after each movement SCF calculations are made until the energy of all system can't drop more. To this energy we call, energy minimization or geometry optimization and allowing to determine structural and electronic features of all the molecules in the system [**25**].

Molecular Mechanics (MM) is simpler and faster than QM since it is based on a potential energy function. It can be used with larger molecules and evaluate the assembly and interaction of multiple molecules such as CyDs [**25**].

Docking small molecules (guests or ligands) with macromolecules (hosts or receptors) was a pioneer method during the beginning of the 1980s decade and remains a highly field of research [**26**]. The molecular docking process tries to predict the structure of the intermolecular complex that is formed between the host and guest molecules. It allows to know the posing[1] of the ligand and be useful primarily as a hit-identification tool [**27**].

[1] process to determine if the conformation and orientation of the ligand fits the active site. It may give many alternative results.

1.5 Aim of this work

In the last decades there has been an enormous increase in the number of studies and publications regarding CyDs. While 30 years ago 4 to 5 CyD papers were published monthly, in the last decade that, on average, has been the number of publications daily. A high number of these publications were dedicated to the study of CyDs inclusion phenomena to be applied in the pharmaceutical sciences field [**13**].

The main goal of this study consists in determining the binding modes of the adducts formed between three natural cyclodextrins, α-, β- and γ-CyD and two derivatives, Me- and Hp-β-CyD, with five anti-asthmatic drugs; salbutamol, the most used short acting β-2 agonist in the treatment of asthma, and four inhaled corticosteroids, a type of drugs applied in the cases with more severe clinical persistence. In this thesis, we investigate the relative stabilities at the quantum level of these adducts and validate our approach with the available data.

Chapter 2

Theory and Methods

2.1 Quantum Mechanics

2.1.1 Schrödinger equation

The Schrödinger formulation (**Equation 2.1**) describes the dynamics of microscopic matter, without time-dependent interactions which happens in the stationary state [**28**].

$$\mathcal{H}\psi = E\psi \tag{2.1}$$

where E is the energy, ψ is the wave function which characterises the particle movement and $\mathcal{H}$ the Hamiltonian operator represented by,

$$\mathcal{H} = -\frac{\hbar^2}{2m}\nabla^2 + V \tag{2.2}$$

the $\hbar$ is the Planck constant divided by 2π, m describes the mass of the electron and ∇^2 called del-squared is a differential operator that represents the partial derivative in three-dimensional cartesian coordinate systems.

The Schrödinger equation cannot be solved for all systems. First of all, it cannot be applied to atoms with more than one electron, so the solutions for polyelectronic atoms or molecules will only be approximated to the real value. This may be due to the different functional forms that the wave function may adopt; another issue to take into account in this multi-electron species is the electron spin, which can have values of $+\frac{1}{2}$ and $-\frac{1}{2}$ at the spin angular momentum [**28**].

2.1.2 Hartree-Fock method

The Hartree-Fock (HF), also known as SCF method, is an approximate method for the determination of the wave function and energy of a quantum many-body system in the stationary state. It was one of the first methods used in the quantum mechanics and the starting point of the post-Hartree-Fock methods and density functional theory (DFT) [**29**].

Nowadays, HF is outdated and presents several limitations. Nevertheless, it was an important milestone for the so called post-Hartree-Fock methods that came after.

2.1.3 Density functional theory

DFT using functionals of electron density introduces a different approach. Instead of calculating the wave function of the electrons, as done in previous methods, it calculates the electronic energy and overall density distribution. DFT is based on the Hohenberg-Kohn models involving a self-consistent approach [**30**]. With the DFT methodology it is necessary to make an approximation due to the exchange-correlation functional, and the treatment of these properties is strongly related with the success of this approach.

Like what happened before, with Planck and others researchers, this method, despite the agreement with experimental results, didn't have a consistent

theory basis compared with the HF method and its post-methods. This led to the development, in the 90s, of the so-called hybrid methods.

2.1.4 Hybrid methods

The hybrid methods are combinations of the exchange term of HF methods with the correlation component of DFT methodology. Thanks to Becke and his discoveries in this field, in the last decades the number of hybrid methods have been increasing significantly [**31**]. One of the most popular exchange-correlation functional is the Becke three-parameter exchange functional [**32**] and the correlation functional Lee, Yang and Parr [**33**] (B3LYP), that with an high accuracy, turn it into a very popular method. The functional used in this work is a hybrid one, called PBE1PBE or PBE0. It is a functional that uses 25% exchange and 75% correlation weighting [**34**] and was derived from the pure functional of Perdew, Burke and Ernzerhof [**35, 36**].

$$E_{xc}^{ACM0} = E_{xc}^{GGA} + \frac{1}{4}(E_x^{HF} + E_x^{GGA}) \tag{2.3}$$

It is a functional well implemented in theoretical studies and has already been used in studies with cyclodextrins [**37**].

2.1.5 Basis set

A basis set in computational chemistry, is a set of basis functions of the atomic orbitals of atoms within a molecule. This theory can be interpreted as restricting the region of space populated by a specific electron.

In the beginning, the Slater-type orbitals were used to describe the molecular orbitals on the basis of linear combinations of atomic orbitals, but unfortunately they were computationally difficult to implement, which prompted and so the Gaussian-type orbitals to be developed. Nowadays, there are hundreds of basis set composed by Gaussian functions [**38**].

A very commonly used basis set is 6-31G. The letter G stands for Gaussian, the number on the left of the hyphen represents the number of primitive Gaussian functions, in this case there were 6, the numbers on the right of the hyphen indicate the number of valence functions. In this case, we have two numbers, so we have a double zeta basis set. The number on the left of the letter G always represent the split 1s orbital of the hydrogen atoms [**28, 38**].

It is also possible to add polarization to this basis sets, allowing the orbitals to change shape. With this, we could have a 6-31G(d) or 6-31G* basis set, which means that d functions were added to the non-hydrogen atoms (heavy atoms). The hydrogen atoms can be polarized too, for instance in the basis set 6-31G(d,p) or 6-31G**, where p functions are added to hydrogen atoms. So, the information inside the parenthesis on the left of the comma, is related to the heavy atoms of the system, while the one on the right regards the hydrogen atoms. In a more complex analysis of a basis set, like 6-31G(2df,2pd), two d functions and one f function were added to the heavy atoms, while two p functions and one d are added to hydrogen atoms [**23**].

Besides polarization, it is also possible to add diffusion to basis sets, especially when dealing with anions and molecules containing lone pairs. These functions allow orbitals to occupy a larger region of space. To use this function on a basis, add a single plus sign right after the G letter, like in 6-31G+(d,p), meaning that the heavy atoms have an extra one s and one p function and when we have two plus signs, not only the heavy atoms have extra functions, but also the hydrogen atoms will have an s diffuse function, as in this example 6-31G++(d,p) [**23**].

2.1.6 Structure Optimization Details

The three dimensional structures of α-, β- and γ-cyclodextrin were obtained in [**39**] while the structures of the anti-asthmatic drugs came from [**40–44**].

The derivatives of the β-CyD were produced adding the necessary groups with PyMOL [**45**].

Before the QM optimization calculations, the structures energy were minimized in the Avogadro software [**46**] with the steepest descent method and with the MMFF94 force field [**47**].

The geometry optimization calculations were done using the Gaussian 09 software package [**48**] with the PBE1PBE functional [**34, 35**] and the basis set 6-31G(d,p) [**38**] for all atoms. The calculations were performed in vacuum with charge equal to zero and multiplicity equal to 1.

Frequency calculations were performed to make sure that the optimized geometries were minima.

All structures were analysed and processed with Chemcraft [**49**] and PyMOL [**45**].

2.2 Molecular Mechanics and Molecular Docking

Molecular mechanics is a nonquantum method, based on an empirical force field, and consists in seeing a molecule as a gathering of particles held together by the elastic forces. Forces that are defined in terms of a potential energy function of internal coordinates such bond lengths, angles and torsion angles, for instance. Diverging from QM, where the electrons are explicitly treated in this method they are implicitly treated.

Within the MM framework, Molecular Docking, is the most commonly used method to determine the best binding sites with as many degrees of freedom as possible and with a realistic evaluation of energy. This method allows the exploration of a large area of the conformational space of the system in study, but requires the use of simple energetic models (the scoring function) to keep computational issues limited [**50**].

2.2.1 Theory

Docking protocols are a combination of search algorithms, exploring all the degrees of freedom of the guest-host system and scoring functions allowing the system to be sampled efficiently, ensuring the detection of the most important binding modes [**26, 27**].

The first algorithms only considered translation and rotation, and treated the ligand and receptor as rigid structures. With the computational evolution and new algorithms, nowadays is possible to treat the ligand with full flexibility and the host as a rigid (or partially flexible) structure [**51**].

2.2.2 The scoring function

Docking usually uses a scoring function based on the approximation of the standard chemical potentials of the system, with Coulomb energies and 6-12 van der Waals interactions that need to be empirically weighted. AutoDock Vina, a new program for molecular docking and virtual screening, has a general form for the conformation dependency in the scoring function,

$$c = \sum_{i<j} f_{t_i t_j}(r_{ij}) \tag{2.4}$$

where the summation is for all the pairs of atoms that can move relatively to each other, excluding 1-4 interactions that are atoms separated by three covalent bonds, consecutively. To each atom i is attributed a type t_i, and a symmetric group of interaction functions $f_{t_i t_j}$ considering an interatomic distance, r_{ij}.

This value can be obtained by the intermolecular and intramolecular contributions:

$$c = c_{inter} + c_{intra} \tag{2.5}$$

The scoring function of Autodock Vina was inspired by X-score [**52**]. The interaction functions $f_{t_i t_j}$ are defined taking into account the surface distance, d_{ij}:

$$d_{ij} = r_{ij} - R_{t_i} - R_{t_j} \tag{2.6}$$

where R_t represents the van der Waals radius of atom type t.

$$f_{t_i t_j}(r_{ij}) \equiv h_{t_i t_j}(d_{ij}) \tag{2.7}$$

In this scoring function, $h_{t_i t_j}$ is the weighted sum of steric interactions, hydrophobic interactions between the hydrophobic atoms and hydrogen bonds, when applied. [**53**].

2.2.3 Molecular Docking Details

For the molecular docking calculations, it was necessary to prepare the initial files and define the running parameters. First, after the initial geometry optimization and assurance of working with minima energy structures, CyDs structures where converted to a PDBQT (Protein Data Bank, partial charge (Q), atom type (T)) file, and all the non-polar atoms where eliminated. The same procedure was applied to the anti-asthmatic drugs, followed by the introduction of flexibility in the covalent bonds. This was done with AutodockTools Version 1.5.6 [**54**].

The docking grids were placed centered on the CyDs hosts and were large enough to allow the exploration of docking solutions on both top and bottom regions of the CyDs. For each system, 50 docking calculations were done providing approximately 20 solutions each, resulting in a total of 1000 docking solutions.

2.3 Structure Permutation and Clustering

The large quantity of docking solutions needed to be grouped in order to identify the preferred binding modes between drugs and CyDs. A problem in these adduct structures is that there is too much artificial variety in the ligand distribution due to symmetry of the CyDs. These host molecules are constituted by several sugar subunits repeats and, therefore, it is possible to obtain the exact same binding mode in different space regions, because the docking software is not able to deal with this symmetry issue. We solved this problem by applying a permutation procedure where the system is rotated periodically one unit at the time. The different root mean square deviation (RMSD) values obtained against a reference structure were evaluated and the smallest value was chosen as it corresponds to the structure closest to the studied space segment. **Figure 2.1a** shows how two very similar docking solutions can appear quite different before the permutation procedure.

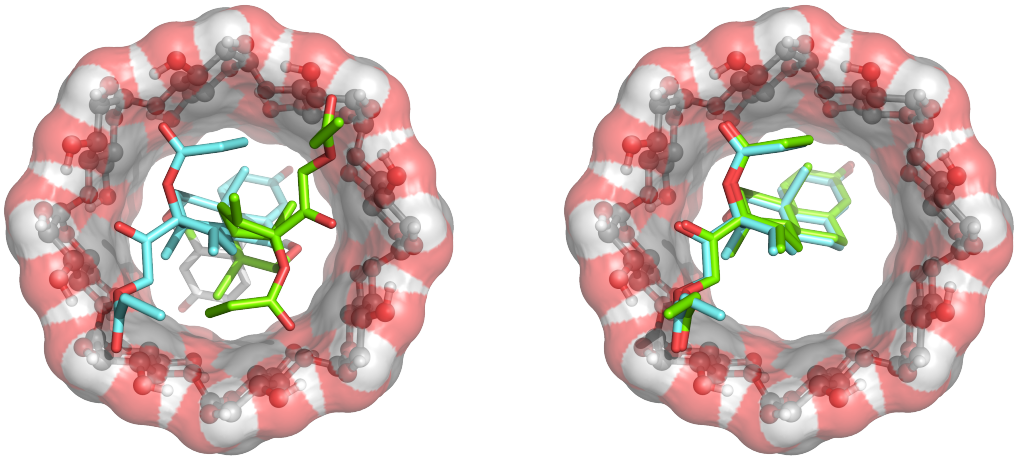

(a) before permutation **(b)** after permutation

Figure 2.1: Structures of two conformations of BEC with γ-CyD before (a) and after (b) permutations.

The permuted docking solutions were then separated in their different binding poses using a clustering procedure. The g_cluster tool from the GROMACS software package [**55**] was used with the Jarvis-Patrick method and

a dissimilarity RMSD cutoff of 0.1 Å. **Figure 2.2** shows several clusters of BEC docked into γ-CyD, sorted by their abundance. The images illustrate the homogeneity within the clusters and the dissimilarity between them. Due to our computational limitations, we had to choose the most representative binding modes to be used in the QM optimization procedures. In the selected conformational clusters, we chose the most representative structures for further studies.

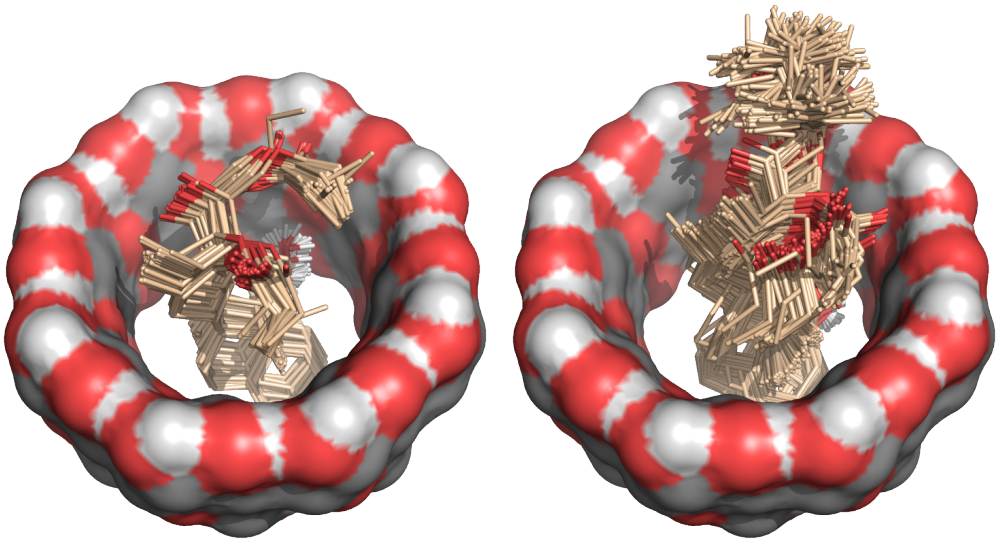

(a) cluster 01 **(b)** cluster 02

Figure 2.2: The clusters obtained from the molecular docking calculations between γ-CyD and BDP. The clusters were sorted by their abundance. *(cont.)*

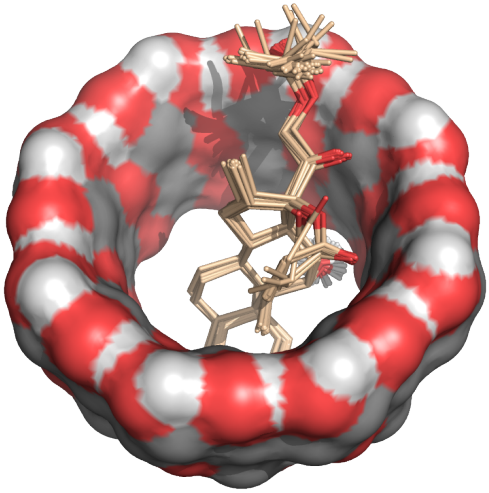

(c) cluster 03

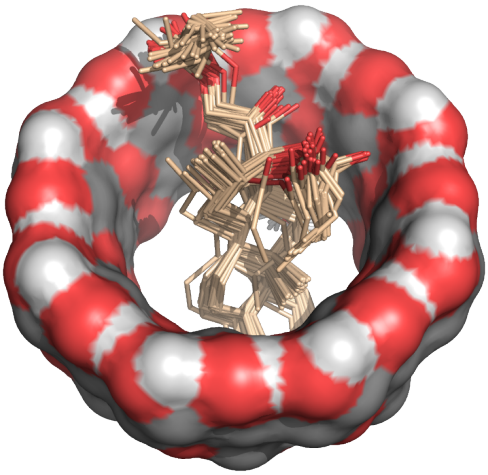

(d) cluster 04

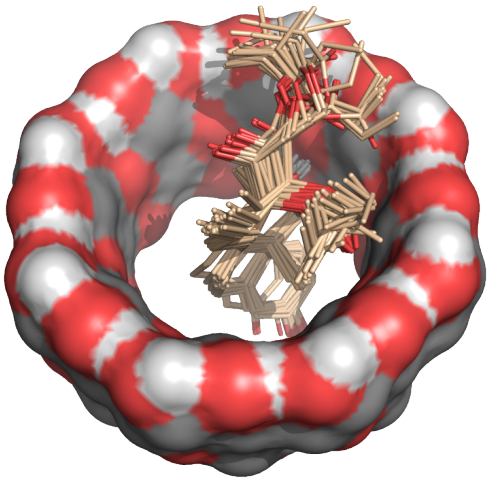

(e) cluster 05

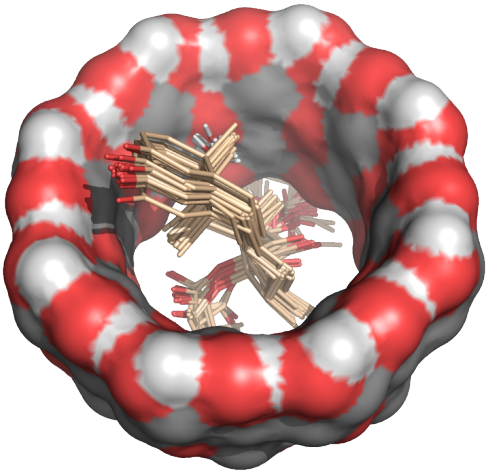

(f) cluster 06

Figure 2.2: The clusters obtained from the molecular docking calculations between γ-CyD and BDP. The clusters were sorted by their abundance. *(cont.)*

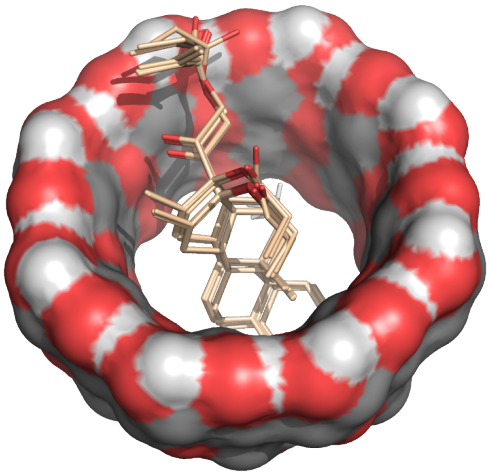

(g) cluster 07

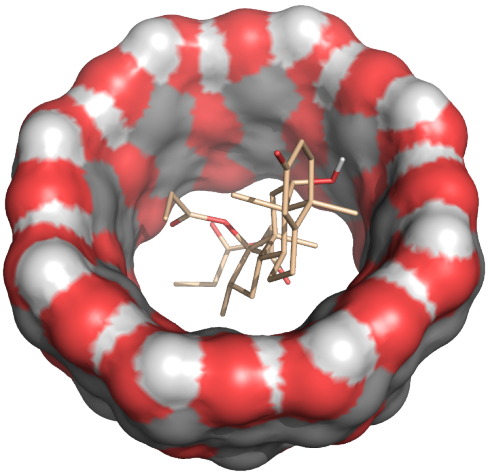

(h) cluster 08

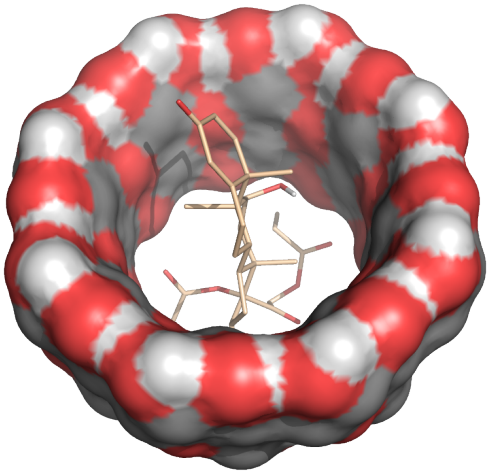

(i) cluster 09

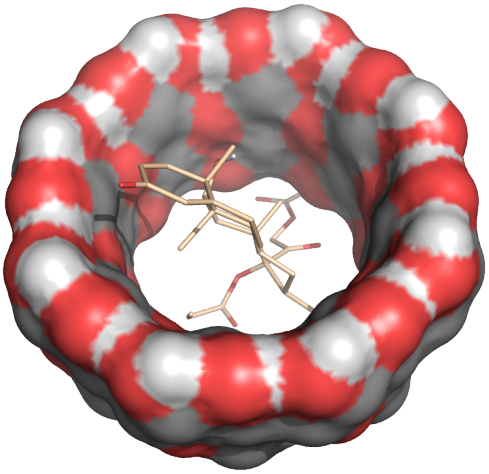

(j) cluster 10

Figure 2.2: The clusters obtained from the molecular docking calculations between γ-CyD and BDP. The clusters were sorted by their abundance.

2.4 Analyses

RMSD is a measurement tool used to evaluate the similarity between two structures. Before the calculation is done, the structures are fitted to each other by rotation and translation, taking into account that one is the reference structure. There are important criteria in the choice of reference structures and the atoms used in the calculations to avoid unwanted results [**56**]. The RMSD can be calculated with the **Equation 2.8**.

$$\mathrm{RMSD} = \sqrt{\frac{1}{M}\sum_{i=1}^{N} m_i d_i^2} \tag{2.8}$$

where M represents the weight of all atoms taken into account in the calculation, m_i is the weight of that specific atom and d_i is the distance in the two structures considered for the RMSD calculation.

All binding energies were calculated according to:

$$\Delta E_{binding} = E_{adduct} - (E_{host} + E_{guest}) \tag{2.9}$$

The enthalpic and Gibbs energies followed the same procedure using the enthalpic and Gibbs energies from the Gaussian output.

All images were rendered using the PyMOL software [**45**].

Chapter 3

Results and Discussion

3.1 Optimized initial structures

3.1.1 Host molecules

In **Figure 3.1** are presented the optimized structures of the CyDs used in this study.

With more subunits available in the structure there is an expected increase in the size of the hosts' cavity. The methyl group presented in the β-CyD derivative may ensure hydrophobicity, while the 2-hydroxypropyl seems to block the lower region of the host (**Figure 3.1**).

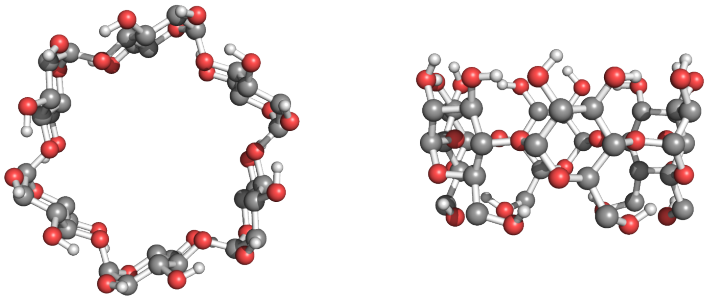

(a) α-CyD

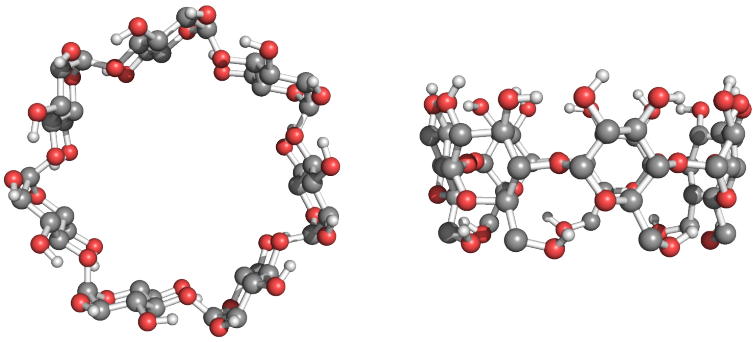

(b) β-CyD

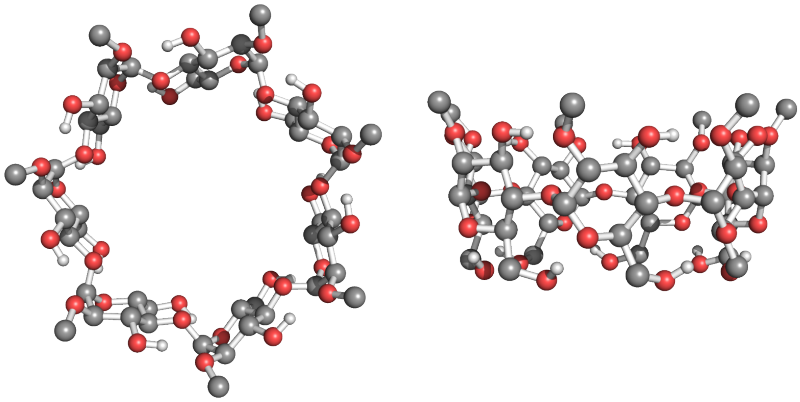

(c) Me-β-CyD

Figure 3.1: Optimized structure of the host molecules. On the left column are the upper view structures and on the right the side view *(cont.)*.

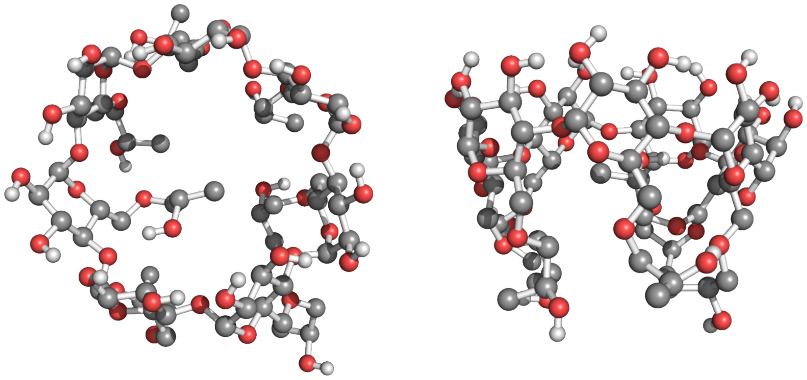

(d) Hp-β-CyD

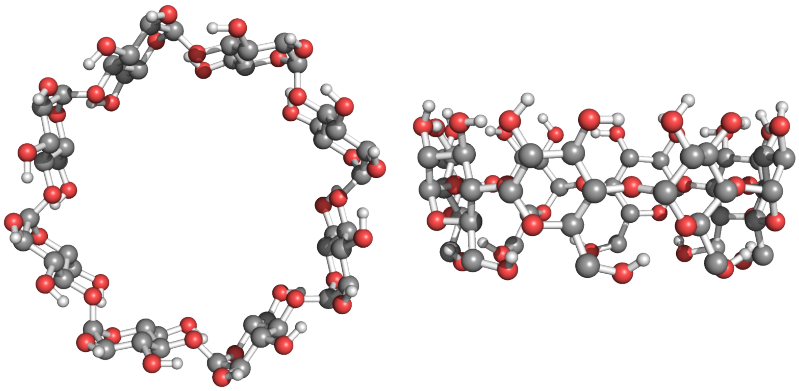

(e) γ-CyD

Figure 3.1: Optimized structure of the host molecules. On the left column are the upper view structures and on the right the side view.

3.1.2 Guest molecules

The anti-asthmatic drugs (guest molecules) were also geometry optimized (**Figure 3.2**).

Four of the five drugs presented have as a core, the corticosteroid group, with the side groups substituted by esther groups (**Figure 3.2a**), hydroxyl and aliphatic groups (**Figure 3.2b**), cyclic aliphatic and esther groups (**Figure 3.2c**) and halogen end atoms (**Figure 3.2d**). These groups will allow the drugs to interact with the hosts quite differently. The 5^{th} guest is

salbutamol, a cyclic aromatic compound with a high polar side and another more hydrophobic (**Figure 3.2e**). SAL is noticeable smaller than the other four drugs and this factor, together with its amphiphilic character, can mediate the interactions with the host molecules.

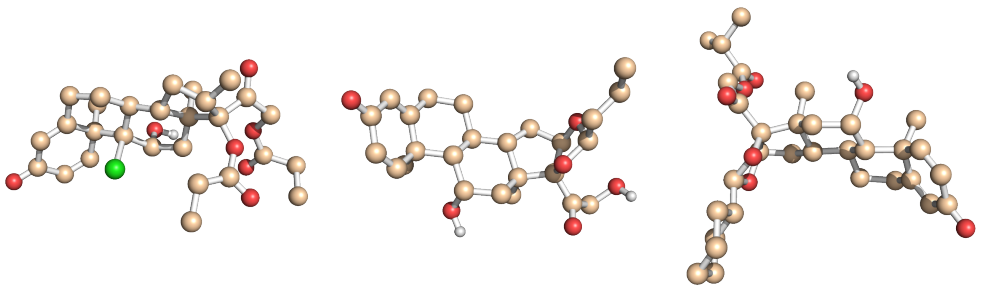

(a) Beclomethasone dipropionate (BDP)

(b) Budesonide (BUD)

(c) Ciclesonide (CIC)

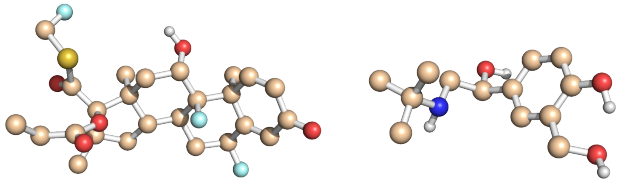

(d) Fluticasone propionate (FP)

(e) Salbutamol (SAL)

Figure 3.2: Optimized structures of the anti-asthmatic drugs.

3.2 Adduct structures

3.2.1 Exploring the best binding modes

Several binding modes were obtained from the molecular docking procedure (see **section 2.2.3**). For each cluster of configurations, we only present the

adduct with lowest energy. The criteria to chose which binding modes were presented and studied further, and which were discarded, was based on both the cluster size (population analysis) and their docking energies. All chosen structures representing the binding modes were structurally optimized at the QM level. Due to the large amount of data generated (too many structures), we only presented the optimized structures of the adducts that change significantly from the molecular docking to the QM calculations.

3.2.1.1 α-cyclodextrin

The molecular docking studies of BDP on α-CyD show two binding modes of interest. In the first case, we have a propionate group inside the cavity (**Figure 3.3a**), while in the other one, the aromatic ring is internalized (**Figure 3.3b**).

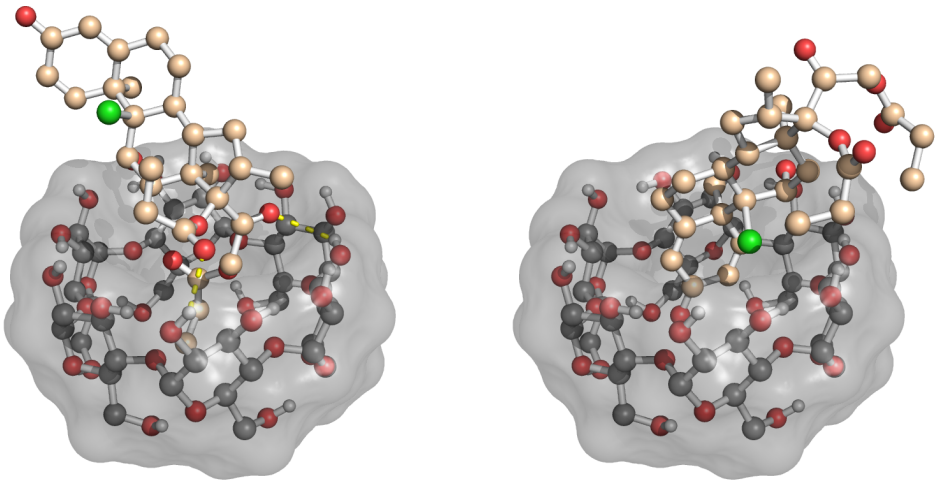

(a) binding mode 1 **(b)** binding mode 2

Figure 3.3: Binding modes between α-CyD and BDP from molecular docking calculations.

After the QM calculations, there was no significant difference in binding mode 1, which tell us that this conformation, from molecular docking, was

close the optimized one. In binding mode 2, it was possible to see a displacement of the guest molecule to the outside and an accommodation in the outer layer leading to interactions between the secondary hydroxyl groups of the CyD and the carbonyl groups of the drug (**Figure 3.4**). This result indicates that binding mode 2 was not a real minimum.

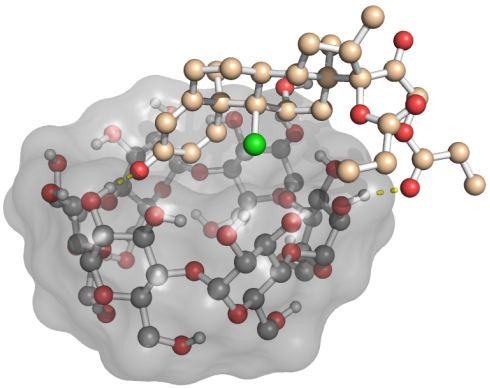

Figure 3.4: Optimized structure of binding mode 2 between α-CyD and BDP after QM calculations.

In the case of the interaction between BUD and α-CyD, there is no clear insertion of the drug in the cavity, and two binding modes were selected, each one with a different side group in the hydrophobic area of the CyD (**Figure 3.5**).

The QM calculation did not change these binding modes, which confirmed the fact that this host is too small for BUD drug.

A similar result was obtained with CIC (**Figure 3.6**), where the drug is only able to insert smaller side groups in the α-CyD cavity.

The QM calculations revealed that, in binding mode 2, and due to the small size of the α-CyD cavity, the cyclic group is slightly displaced outside the CyD, not as much as what was seen in binding mode 2 of BDP, but enough to observe a bending behavior of the aromatic ring in one side of the adduct,

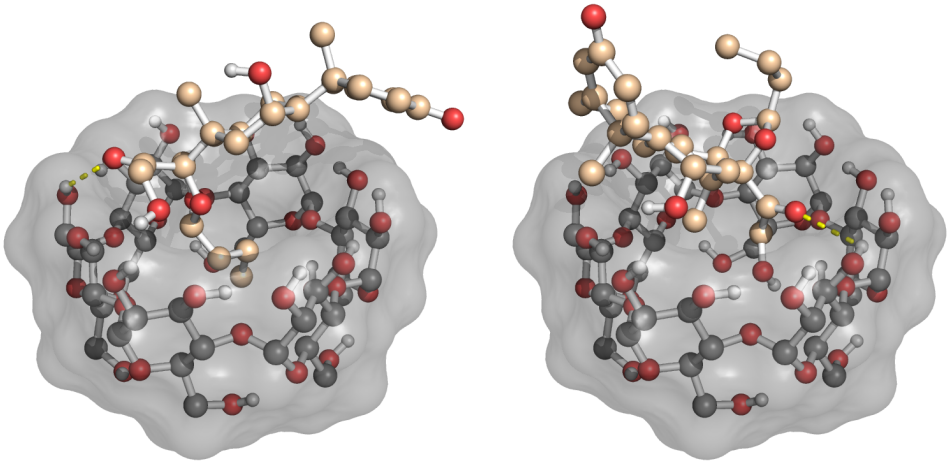

(a) binding mode 1 **(b)** binding mode 2

Figure 3.5: Binding modes between α-CyD and BUD from molecular docking calculations.

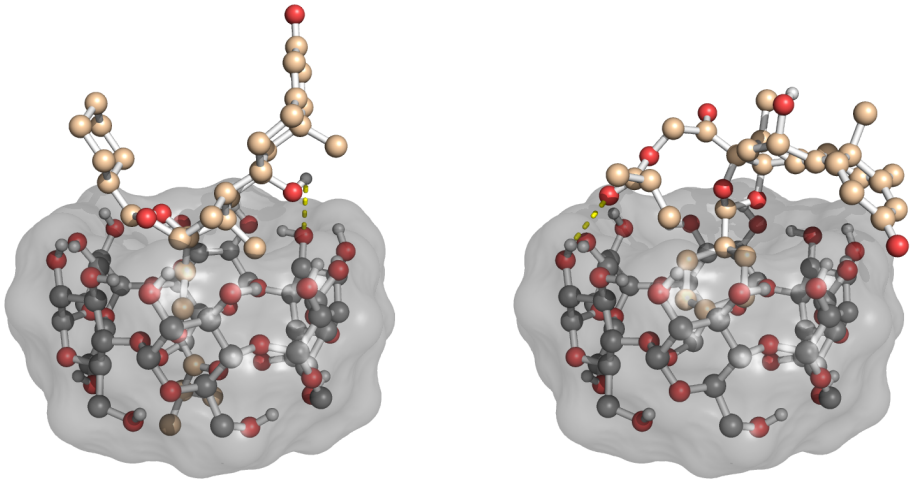

(a) binding mode 1 **(b)** binding mode 2

Figure 3.6: Binding modes between α-CyD and CIC from molecular docking calculations.

an approximation of the carbonyl of the esther group and the oxygen in the ring to the secondary hydroxyl groups of the host (**Figure 3.7**).

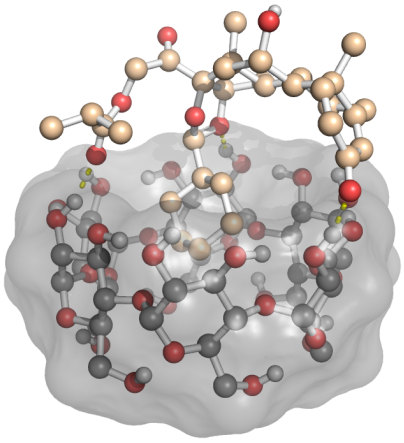

Figure 3.7: Optimized structure of binding mode 2 between α-CyD and CIC after QM calculations.

FP was the last corticosteroid drug studied in an adduct with α-CyD. In this case, three promising binding modes were selected from the molecular docking calculations (**Figure 3.8**). This drug displaced a variety of binding modes when complexing with the α-CyD. In the first binding mode, the drug in a vertical position from the carbonyl group of the cyclic part until the fluor atom, with most of the molecule outside of the cavity and the esther group near the upper side of the host (**Figure 3.8a**). In another conformation, the same structure that was upright is now parallel covering the upper surface while the esther group is inside the cavity (**Figure 3.8b**), and in a last geometry, we observe a significant part of the molecule inside the cavity with the side groups near the CyD hydroxyl groups (**Figure 3.8c**).

The QM calculations had significative impact on the binding modes that showed a partial insertion of the linear group with an ending fluor atom and the corticosteroid group on α-CyD (binding modes 1 and 3). In the first binding mode, a structural relaxation leads the carbonyl group of the esther

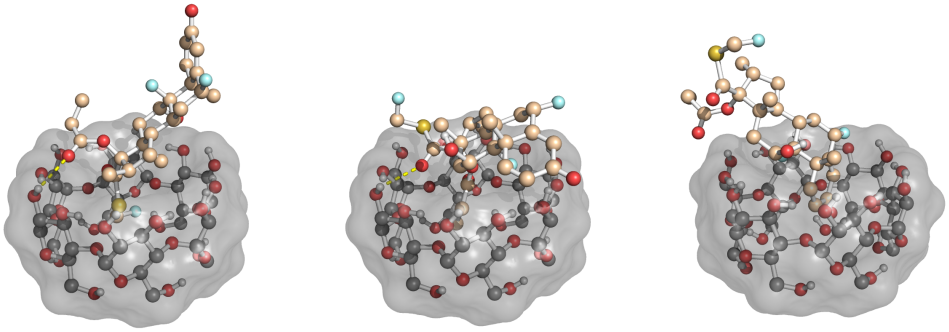

(a) binding mode 1 **(b)** binding mode 2 **(c)** binding mode 3

Figure 3.8: Binding modes between α-CyD and FP from molecular docking calculations.

and the hydroxyl of the corticosteroid group to approach the secondary hydroxyl groups of the upper layer, while the distribution inside the cavity is not affected (**Figure 3.9a**). In binding mode 3, the aromatic ring inside the CyD gets expelled from the cavity leading the carbonyl group of the esther to approach the hydroxyl groups of the layer (**Figure 3.9b**).

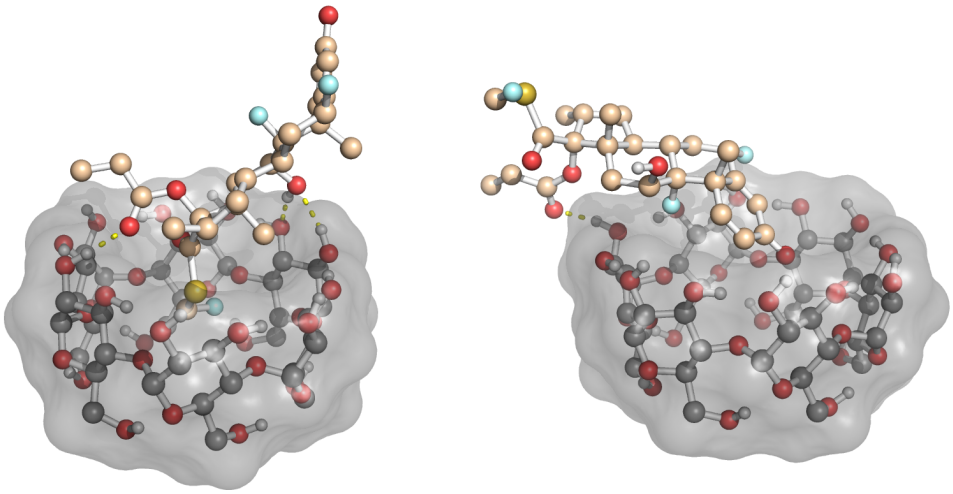

(a) binding mode 1 **(b)** binding mode 3

Figure 3.9: Optimized structures of binding mode 1 and 3 between α-CyD and FP after QM calculations.

The non-corticosteroid SAL drug, due to its smaller size and functional groups, was able to interact with α-CyD through inclusion and non-inclusion adducts (**Figure 3.10**). In binding mode 1, we observe a complete inclusion of the drug, with the primary and secondary hydroxyl groups facing the upper side of the CyD (**Figure 3.10a**). The binding mode 2 is a non-inclusion adduct, with only one hydroxyl group inserted in the cavity (**Figure 3.10b**).

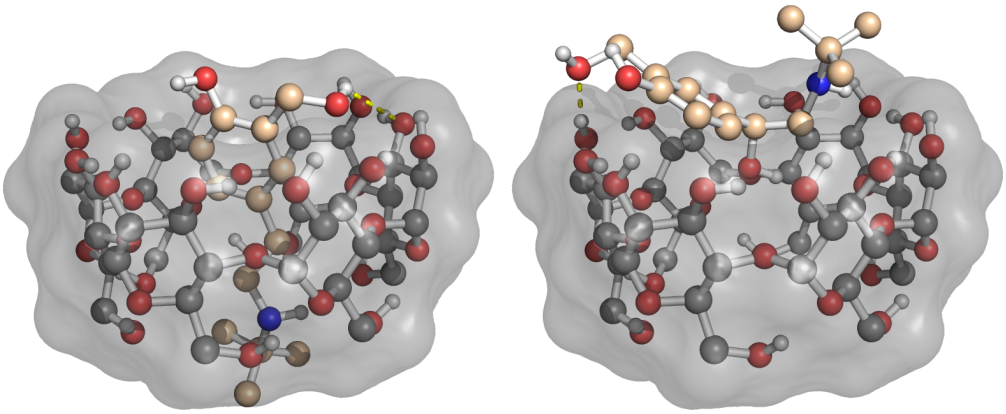

(a) binding mode 1 **(b)** binding mode 2

Figure 3.10: Binding modes between α-CyD and SAL from molecular docking calculations.

The QM optimization confirmed that binding mode 1 with the complete insertion was stable and corresponded to a minimum. However, in binding mode 2, it was observed a rearrangement of the hydroxyl groups of the guest, favoring both inter- and intramolecular hydrogen bonds (**Figure 3.11**).

In conclusion, α-CyD does not seem a good host to form inclusion adducts with the larger corticosteroid drug molecules. As a consequence, it probably forms less stable adducts too dependent on specific interactions with its secondary hydroxyl groups.

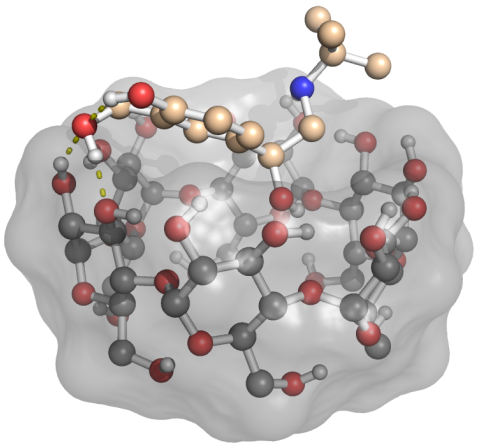

Figure 3.11: Optimized structure of binding mode 2 between α-CyD and SAL after QM calculations.

3.2.1.2 β-cyclodextrin

In β-CyD there is one extra subunit available in the structure, what increases its cavity diameter (hydrophobic area). The interaction of this CyD with the BDP drug resulted in three preferential binding modes, two of them with inclusion type adducts (**Figure 3.12**).

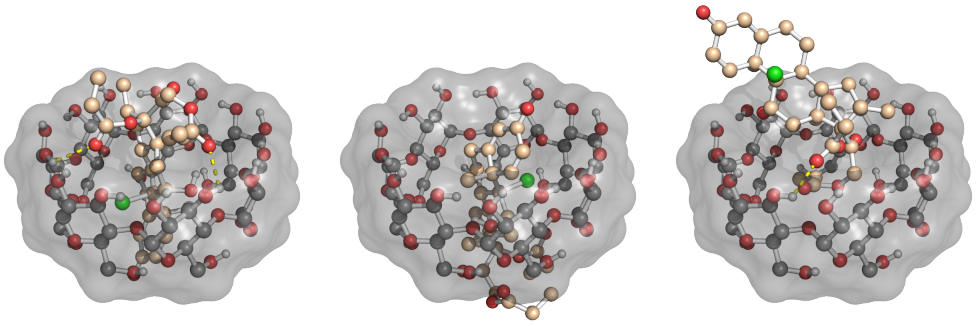

(a) binding mode 1 **(b)** binding mode 2 **(c)** binding mode 3

Figure 3.12: Binding modes between β-CyD and BDP from molecular docking calculations.

After geometry optimization with QM calculations, the adduct structures proved to be stable minima with only some local relaxation observed. These binding modes with full insertion indicate that cavity size is no longer a limitation and that the stability of the adduct will come most probably from the complementarity between drug and CyD.

With the BUD drug, also three binding modes where obtained (**Figure 3.13**). The first two are inclusion adducts with the main functional group of the corticosteroid inside the cavity, differing only in the fact that they are inverted (**Figures 3.13a** and **3.13b**), while binding mode 3 is a non-inclusion complex with the guest spanned horizontally across the upper region of the CyD (**Figure 3.13c**).

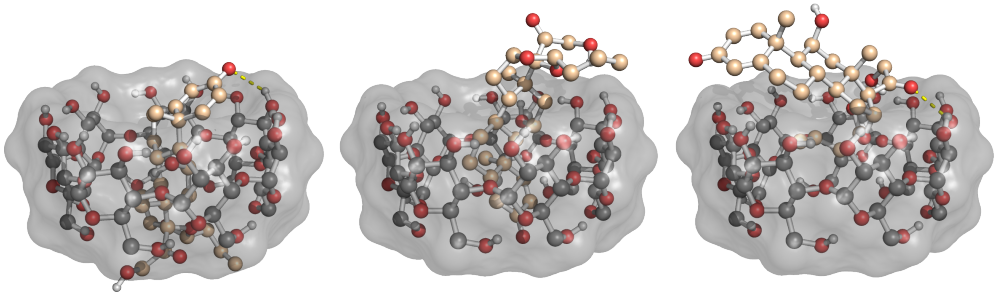

(a) binding mode 1 **(b)** binding mode 2 **(c)** binding mode 3

Figure 3.13: Binding modes between β-CyD and BUD from molecular docking calculations.

In the QM calculations, the first binding mode undergoes a significant re-organization even though the drug remains completely inserted. The main carbonyl group approaches the secondary hydroxyl groups of β-CyD and this bending effect leads to other interactions between the primary hydroxyl groups of guest and host (**Figure 3.14**). This was observed between the carbonyl end of the corticosteroid and the secondary hydroxyl group side (and not with the primary), probably because in this case there are two acceptors available per subunit, instead of one.

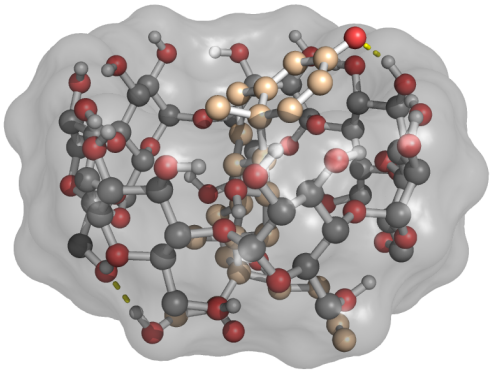

(a) binding mode 1

Figure 3.14: Optimized structure of binding mode 1 between β-CyD and BUD after QM calculations.

The two binding modes obtained with CIC showed the corticosteroid molecule interacting with CyD's cavity even though a complete insertion was not observed (**Figure 3.15**). The QM calculations confirmed these binding modes and also confirmed that a larger insertion is still limited by the cavity size of this CyD.

The docking calculations with FP resulted in three different binding modes (**Figure 3.16**). In the first case, we have an inclusion adduct with the carbonyl of the functional group facing the top side of the CyD as can be seen in **Figure 3.16a**. In the other two cases the guest is in an inverted position with different levels of insertion. The binding mode 2 is a perfect example of the guest in full inclusion (**Figure 3.16b**). However, in binding mode 3, we have a lower level of insertion, with the aromatic ring of the corticosteroid remaining in the internal hydrophobic region of β-CyD, while the other groups are interacting with the secondary hydroxyl groups of the host (**Figure 3.16c**).

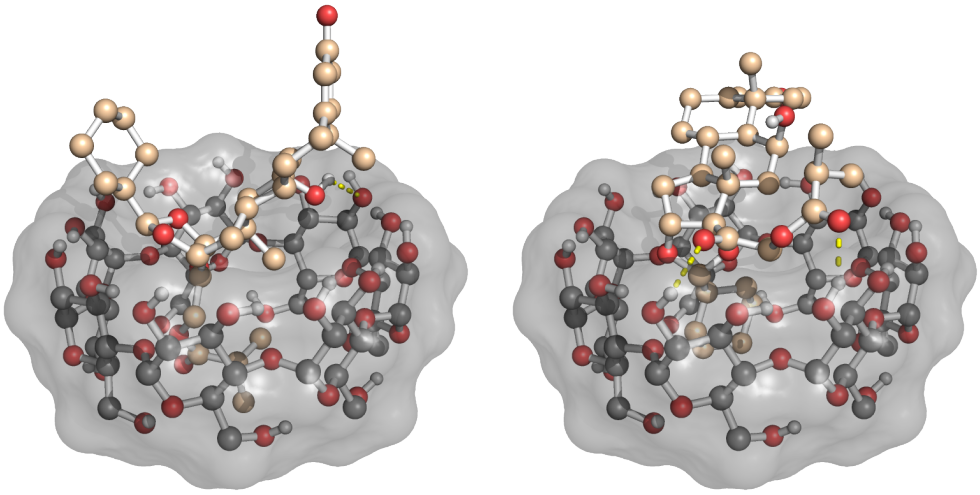

(a) binding mode 1 **(b)** binding mode 2

Figure 3.15: Binding modes between β-CyD and CIC from molecular docking calculations.

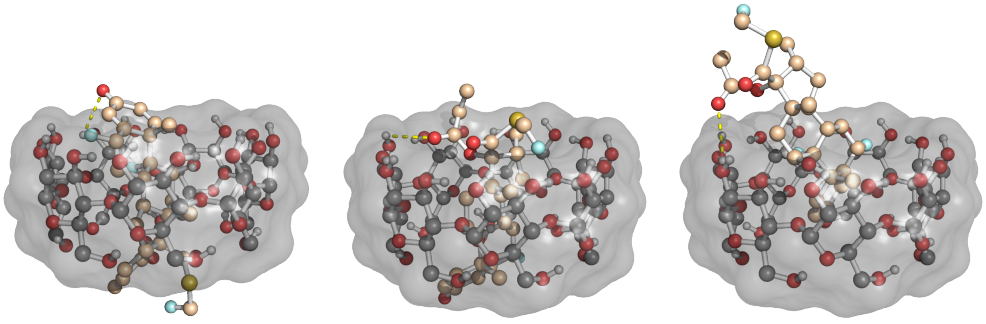

(a) binding mode 1 **(b)** binding mode 2 **(c)** binding mode 3

Figure 3.16: Binding modes between β-CyD and FP from molecular docking calculations.

The QM calculations led to significant changes to binding mode 1 and 3, favoring interactions between the hydroxyl groups. **Figure 3.17a** shows the newly formed hydrogen bonds between the carbonyl group in FP and the secondary hydroxyl layer of CyD, and between an hydroxyl group of the corticosteroid group and the primary hydroxyl group in the other layer of the CyD. **Figure 3.17b** shows a large displacement of the guest to the outside, favoring the formation of the hydrogen bond interactions at the top side of CyD, but also showing that the partial insertion present in this binding mode was not stable enough.

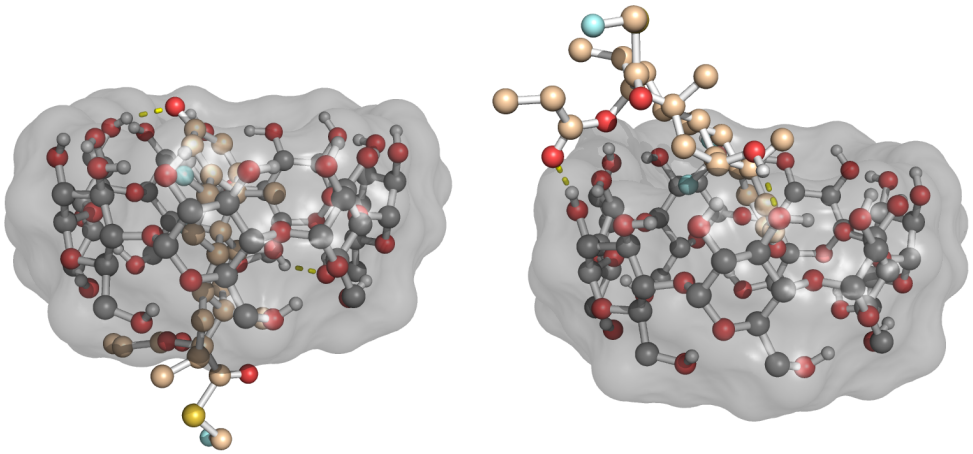

(a) binding mode 1 **(b)** binding mode 3

Figure 3.17: Optimized structures of binding mode 1 and 3 between β-CyD and FP after QM calculations.

The smaller SAL drug does not have much steric hindrance when interacting with β-CyD. In fact, the two main binding modes present two full insertions of the drug only varying its orientation (upside down) regarding the top face of the CyD (**Figure 3.18**).

The QM calculations revealed significant rearrangements in both binding modes. Binding mode 1, in the wider side of the host, undergoes a rearrangement leading to a network of hydrogen bonding between two hydroxyl groups of the host and the primary and secondary hydroxyl groups of SAL

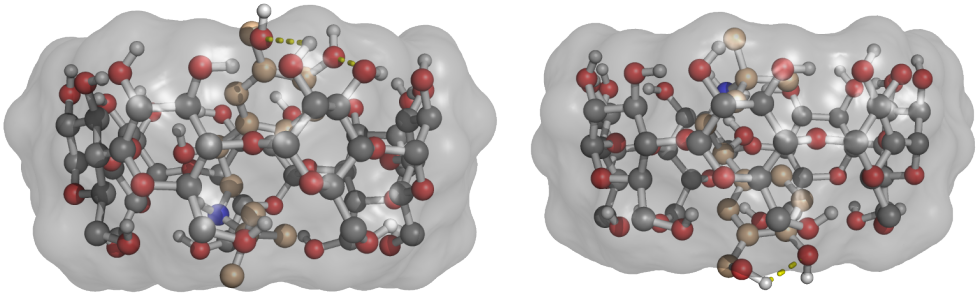

(a) binding mode 1 **(b)** binding mode 2

Figure 3.18: Binding modes between β-CyD and SAL from molecular docking calculations.

(**Figure 3.19a**). In binding mode 2, we observe that the intramolecular hydrogen bond network of the host reshuffles to introduce the secondary hydroxyl group of SAL and allowing also the primary group to work as an hydrogen bond donor (**Figure 3.19b**).

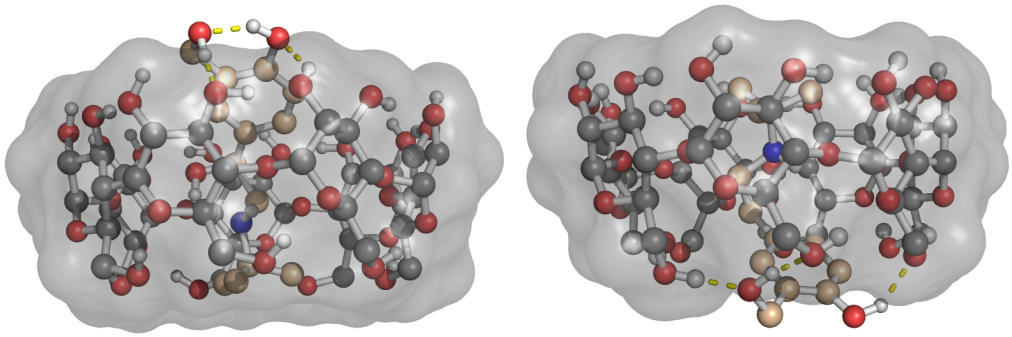

(a) binding mode 1 **(b)** binding mode 2

Figure 3.19: Optimized structures of binding mode 1 and 2 between β-CyD and SAL after QM calculations.

In general, β-CyD gives rise to a larger variety of binding modes and an higher level of inclusion of guest molecules comparing with α-CyD.

3.2.1.3 Methyl-β-cyclodextrin

Figure 3.20 presents the adducts formed between the Me-β-CyD and the BDP drug. The first binding mode has the carbonyl end of the corticosteroid group directed to the narrow part of the host while the propionate groups are in the wider top part in a good degree of inclusion (**Figure 3.20a**). This binding mode presents large similarities with the 1^{th} binding mode between BDP and β-CyD (**Figure 3.12a**). The binding mode 2, has the propionate groups inside the CyDs' cavity while the corticosteroid group is outside of the wider part of the host (**Figure 3.20b**). This binding mode is also quite similar to the the third binding mode of this drug and β-CyD. These similarities suggest that the extra methyl group does not affect significantly the binding of BDP. After QM calculations, both structures maintained their configurations without major changes.

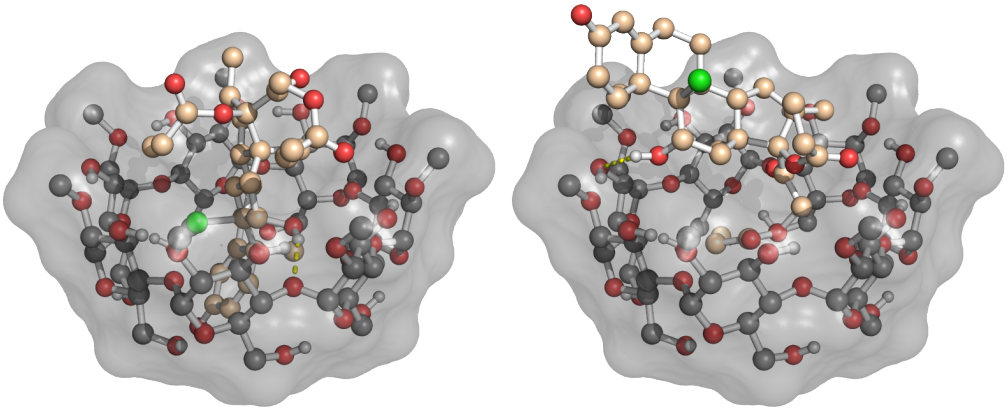

(a) binding mode 1 **(b)** binding mode 2

Figure 3.20: Binding modes between Me-β-CyD and BDP from molecular docking calculations.

In the study with BUD three binding modes were identified with molecular docking (**Figure 3.21**). The first binding mode is a insertion with the carbonyl end in the narrow side of the host and the aliphatic and hydroxyl

groups in the wider side (**Figure 3.21a**). In the second and third binding modes, we have either the hydroxyl group (**Figure 3.21b**) or this and the aliphatic group (**Figure 3.21c**), inside the cavity with the remaining groups oriented near the methyl and secondary hydroxyl groups of the CyD. Just like previous QM optimizations with this CyD, there were no significant changes after these calculations.

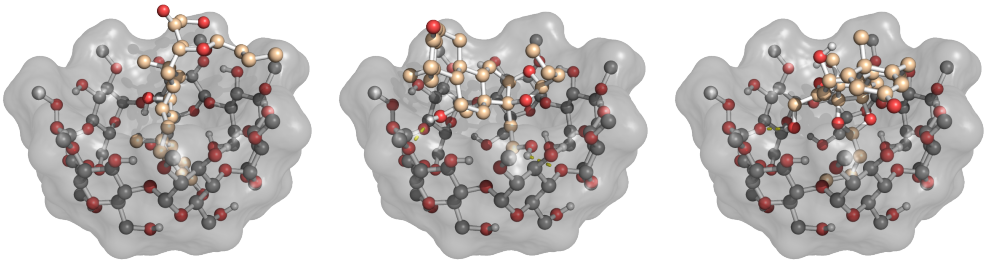

(a) binding mode 1 **(b)** binding mode 2 **(c)** binding mode 3

Figure 3.21: Binding modes between Me-β-CyD and BUD from molecular docking calculations.

In the study of the pro-drug CIC with Me-β-CyD, we also obtained three different binding modes (**Figure 3.22**). These modes are characterized by individual insertions of the three groups composing the drug molecule while the remaining ones stay in the wider region of the host. In the first case we have the propionate group inside the cavity (**Figure 3.22a**), in the second is the aliphatic cyclic group (**Figure 3.22b**) and in the last, the corticosteroid group inserts in the cavity (**Figure 3.22c**). From these adducts, the last one was shown not to be very stable, as its configuration was significantly changed after QM optimization (**Figure 3.23**). The corticosteroid group inside the host was displaced to the wider side of the CyD, resulting in an adduct almost with any insertion.

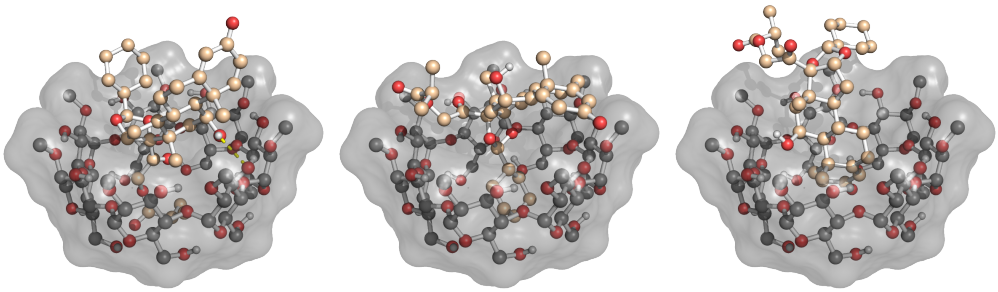

(a) binding mode 1 **(b)** binding mode 2 **(c)** binding mode 3

Figure 3.22: Binding modes between Me-β-CyD and CIC from molecular docking calculations.

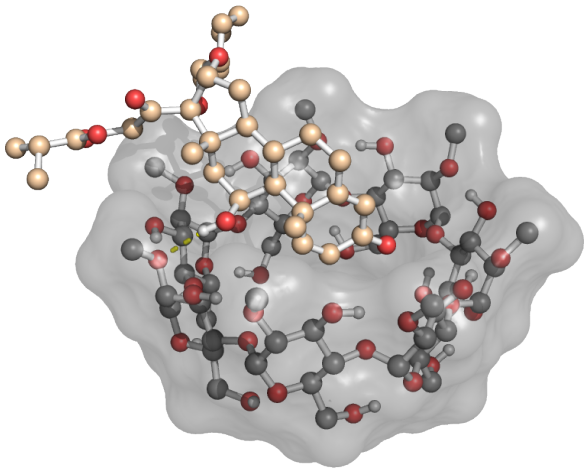

Figure 3.23: Optimized structure of binding mode 3 between Me-β-CyD and CIC after QM calculations.

The last corticosteroid drug studied was FP, where we identified four binding modes with Me-β-CyD (**Figure 3.24**). The first two binding modes are opposite to each other where the carbonyl end of the corticosteroid is in the wider and the remaining groups arranged in the narrow side (**Figure 3.24a**), and vice-versa (**Figure 3.24b**). The third binding mode is similar to the second but without such a good degree of encapsulation of the guest (**Figure 3.24c**). In the last binding mode, the terminal fluor atom is located in the hydrophobic area of the CyD with the other two groups in the methyl and hydroxyl groups side (**Figure 3.24d**). QM calculations confirmed that binding modes 1, 2 and 4 were stable. However, binding mode 3 changed significantly with the displacement of the aromatic ring from the cavity and arrangement the remaining groups in the wider side, allowing the only hydroxyl group of the guest to hydrogen bond with the secondary hydroxyl group of the host (**Figure 3.25**).

With SAL interacting with Me-β-CyD, two binding modes were identified. In both binding modes the drug is completely encapsulated in the host, one with the hydroxyl groups of the ring pointing to the wider side, while the methyl group is in the narrow side of the CyD (**Figure 3.26a**). In the other binding mode these interaction points are inverted (**Figure 3.26b**). The QM optimization revealed a series of structural reorganizations to both binding modes (**Figure 3.27**). In both cases SAL is able to form an intramolecular hydrogen bond between its two hydroxyl groups. However, while in binding mode 1, both groups interact with the host (**Figure 3.27a**) in binding mode 2 only one is able to do this interaction (**Figure 3.27b**).

The extra methyl group in Me-β-CyD created an extra difficulty for most drugs to interact with this host, as it decreases the ability of the host to act as an hydrogen bond donor. The increased hydrophobicity can play a role in the affinity towards this host but, at the moment, we only observed a decrease in the specificity.

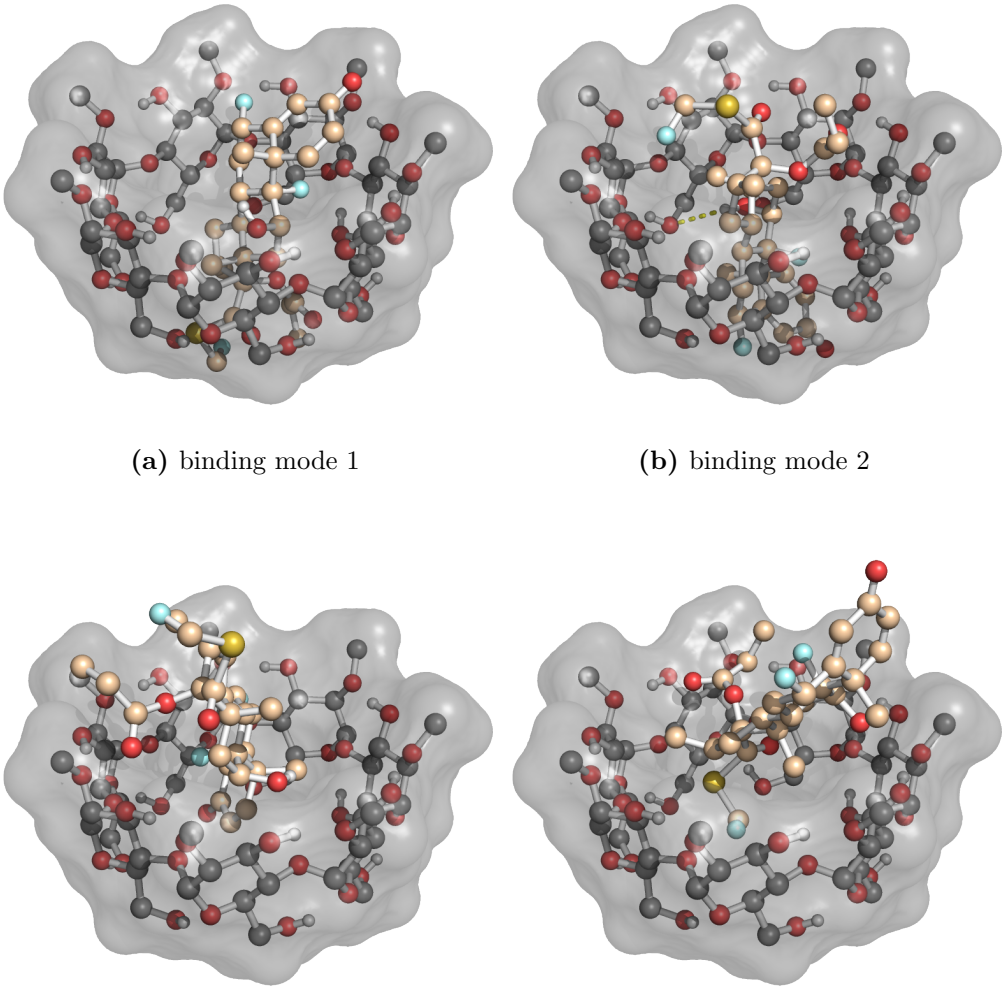

(a) binding mode 1

(b) binding mode 2

(c) binding mode 3

(d) binding mode 4

Figure 3.24: Binding modes between Me-β-CyD and FP from molecular docking calculations.

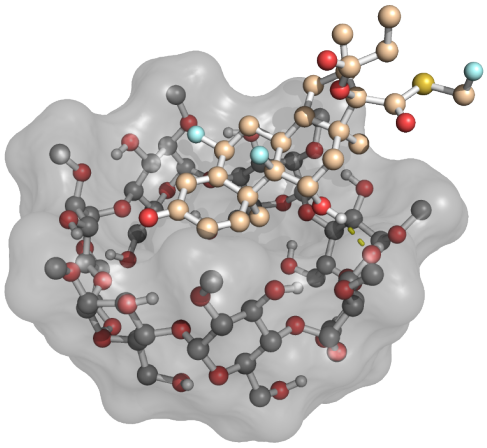

Figure 3.25: Optimized structure of binding mode 3 between Me-β-CyD and FP after QM calculations.

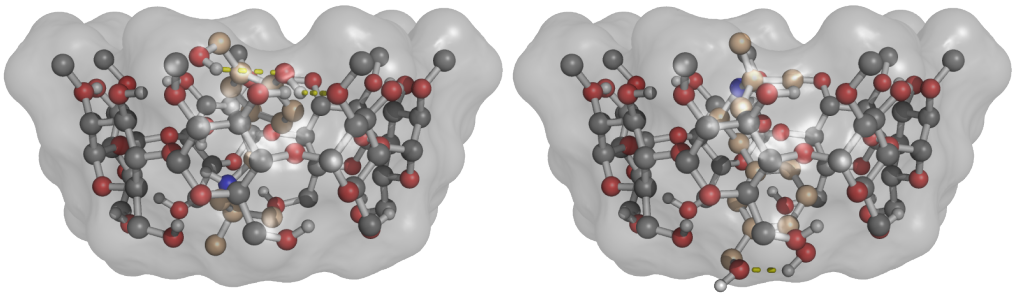

(a) binding mode 1 **(b)** binding mode 2

Figure 3.26: Binding modes between Me-β-CyD and SAL after molecular docking calculations.

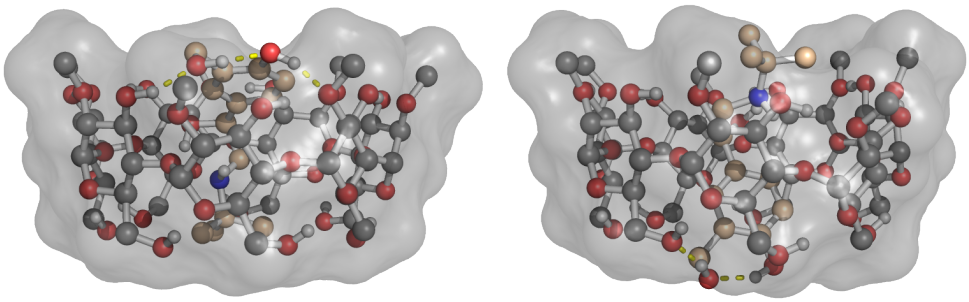

(a) binding mode 1 **(b)** binding mode 2

Figure 3.27: Optimized structures of binding mode 1 and 2 between Me-β-CyD and SAL after QM calculations.

3.2.1.4 2-hydroxypropyl-β-cyclodextrin

The first drug studied with this derivative of β-CyD was BDP and three binding modes were identified. One with a propionate group inside the cavity and the remaining groups organized in the wider side of the host (**Figure 3.28b**) and the other two binding modes with different levels of insertion of the corticosteroid group. While in binding mode 1 the inclusion of the corticosteroid group is deep, near the hydroxyl of the propyl group of the host (**Figure 3.28a**), the inclusion in binding mode 3 is shallow, remaining near the aromatic rings of the Hp-β-CyD (**Figure 3.28c**). It seems that with this substitution on the primary hydroxyl groups of the host, the hydrophobicity of the cavity goes beyond the aromatic rings of the CyD's subunits, reaching the region of the hydroxypropyl groups. The QM calculations showed some changes in the arrangement of the host propyl groups but significant changes could only be observed in binding mode 1. In **Figure 3.29**, we see the final configuration of this binding mode, with a hydrogen bond between the end carbonyl of the corticosteroid group and the

secondary hydroxyl of the propyl group. This type of interaction is similar to what we observed with the primary hydroxyl groups of β-CyD, but in the case of Hp-β-CyD the guest molecule inserts much deeper allowing all the cyclic rings to be encapsulated in the cavity.

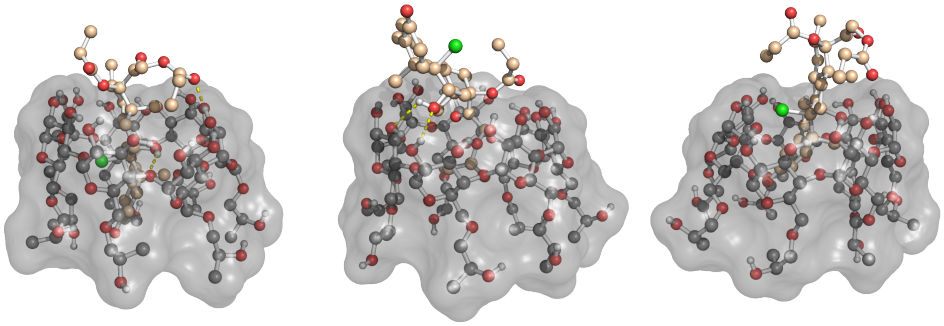

(a) binding mode 1 **(b)** binding mode 2 **(c)** binding mode 3

Figure 3.28: Binding modes between Hp-β-CyD and BDP after molecular docking calculations.

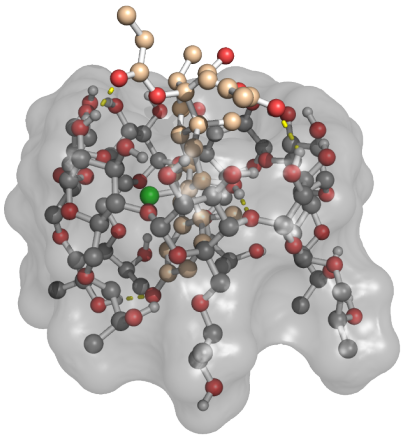

Figure 3.29: Optimized structure of binding mode 1 between Hp-β-CyD and BDP after QM calculations.

We identified four binding modes between BUD and Hp-β-CyD (**Figure 3.30**). Binding mode 1 is fully inserted in the host, with the carbonyl end

group near the secondary hydroxyl groups and the aliphatic and hydroxyl end groups near the hydroxypropyl substitute in the narrow side (**Figure 3.30a**). In binding mode 3, we only have insertion of the aliphatic linear group with the remaining groups arranged in the wider side (**Figure 3.30c**). Binding modes 2 and 4 differ mainly on the level of insertion, with one much more encapsulated than the other, respectively (**Figures 3.30b** and **3.30d**). The QM calculations confirmed that these binding modes were very close to minima configurations. Nevertheless, binding modes 2 and 3 (**Figure 3.31**) underwent structural rearrangements to favor the formation of hydrogen bonds between the hydroxyl and carbonyl groups of the drug and the secondary hydroxyl groups of Hp-β-CyD.

We identified two binding modes between CIC and Hp-β-CyD. In one case, the aliphatic cyclic ring is inside the host's cavity (**Figure 3.32a**), while the other binding mode has the propionate group inserted (**Figure 3.32b**). Both binding modes show most of the drug in a very shallow position with only partial insertion. The QM calculations did not result in significant changes to the docking binding modes.

We identified two binding modes between FP and Hp-β-CyD with completely opposite orientations. In **Figure 3.33a** we observe binding mode 1 where the guest molecule is encapsulated in the host with the carbonyl end group near the hydroxypropyl groups of the host and the remaining groups near the secondary hydroxyl groups in the wider side. In binding mode 2 the opposite orientations are observed with the carbonyl end group in the wider side and the other two groups inside the cavity near the hydroxypropyl groups (**Figure 3.33b**). The QM optimizations confirmed that these were indeed stable structures.

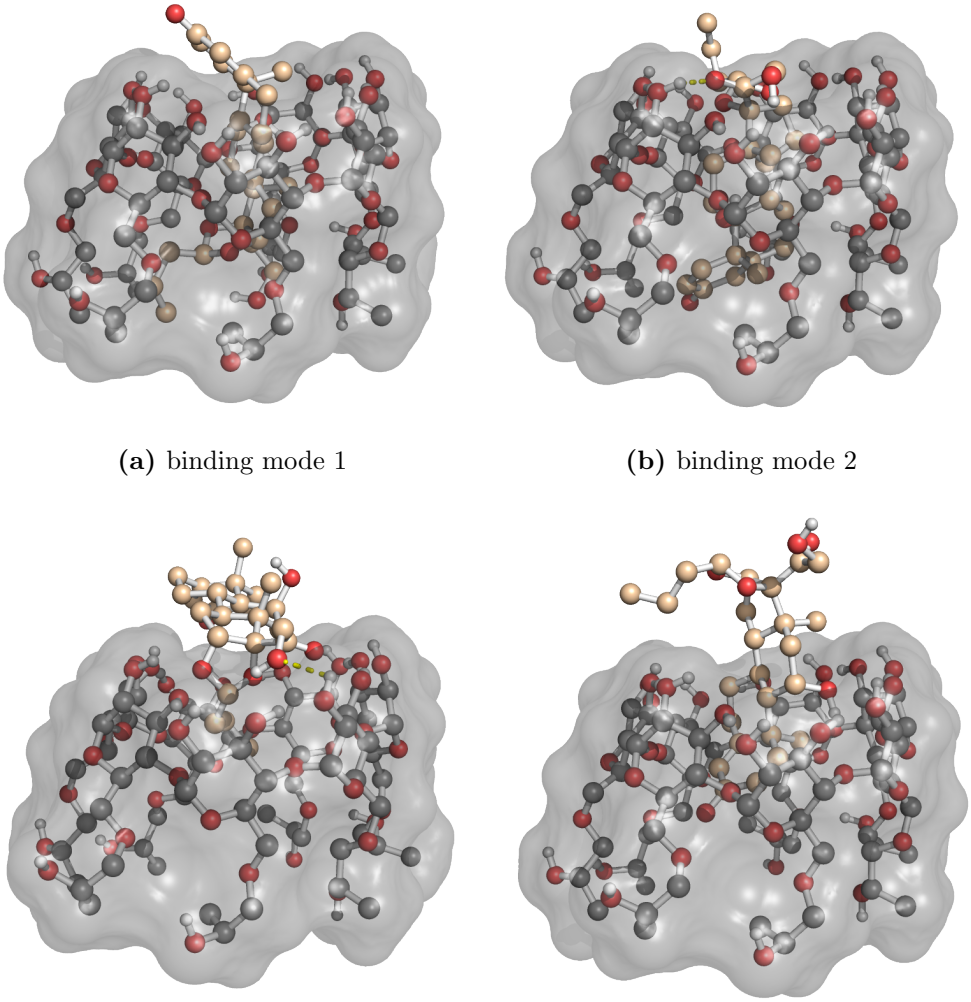

(a) binding mode 1

(b) binding mode 2

(c) binding mode 3

(d) binding mode 4

Figure 3.30: Binding modes between Hp-β-CyD and BUD after molecular docking calculations.

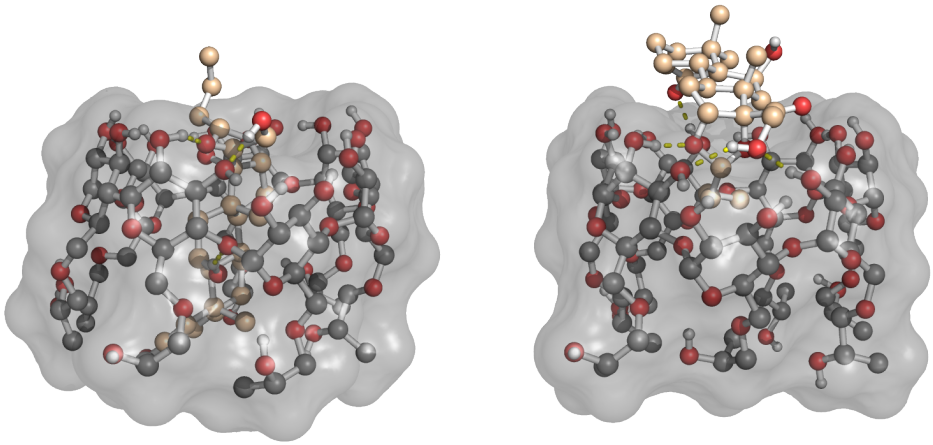

(a) binding mode 2 **(b)** binding mode 3

Figure 3.31: Optimized structures of binding mode 2 and 3 between Hp-β-CyD and BUD after QM calculations.

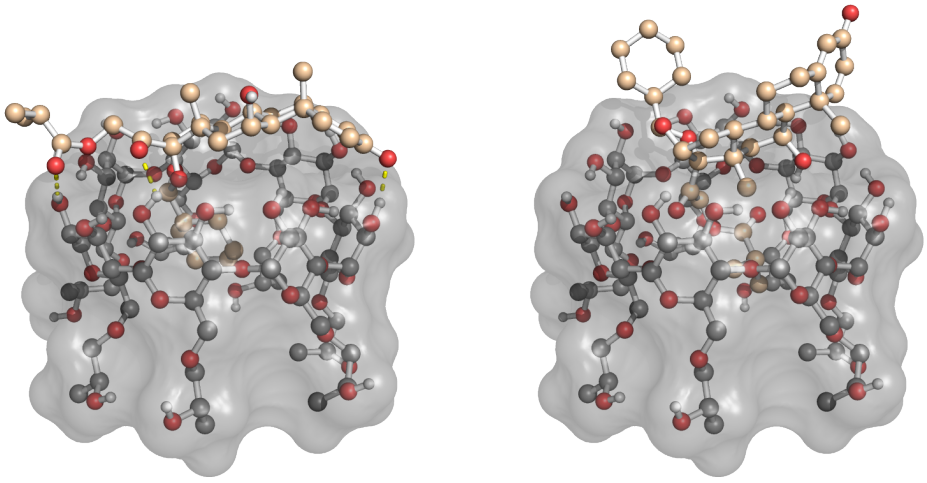

(a) binding mode 1 **(b)** binding mode 2

Figure 3.32: Binding modes between Hp-β-CyD and CIC after molecular docking calculations.

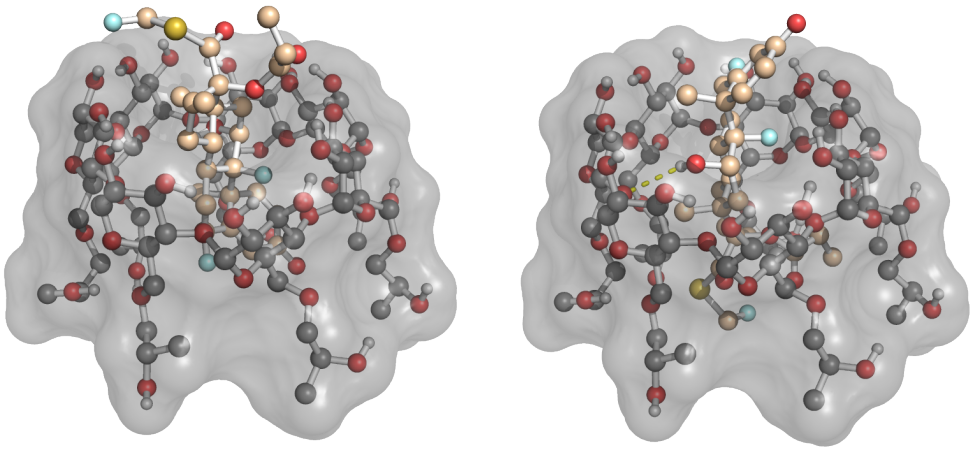

(a) binding mode 1 **(b)** binding mode 2

Figure 3.33: Binding modes between Hp-β-CyD and FP after molecular docking.

The docking study between SAL and Hp-β-CyD revealed three binding modes. The first two binding modes have the primary and secondary hydroxyl groups near the wider side of the host and the methyl group inside the cavity. However, they change in the degree of insertion with binding mode 1 more encapsulated (**Figure 3.34a**) than binding mode 2 (**Figure 3.34b**). In binding mode 3, the guest molecule is inverted, compared with the previous two binding modes, with the hydroxyl groups inside the cavity and the methyl near the top hydroxyl groups of the host (**Figure 3.34c**). The QM calculations revealed significant rearrangements, favoring the hydrogen bond formation. In the first binding mode, the secondary hydroxyl group in the guests' aromatic ring makes an intramolecular hydrogen bond with the nearby primary hydroxyl group. This group and the other secondary hydroxyl in the molecule also underwent intermolecular hydrogen bonding in the wider side of the host and inside the cavity, respectively (**Figure 3.35a**). **Figure 3.35b** shows in the wider side, the hydroxyl groups establishing intermolecular hydrogen bonds with the host. In the last binding mode, which is inverted, we have an intramolecular hydrogen bond between

the hydroxyl groups of the guest and intermolecular hydrogen bonds of the secondary hydroxyl group inside the cavity and the hydroxypropyl group (**Figure 3.35c**).

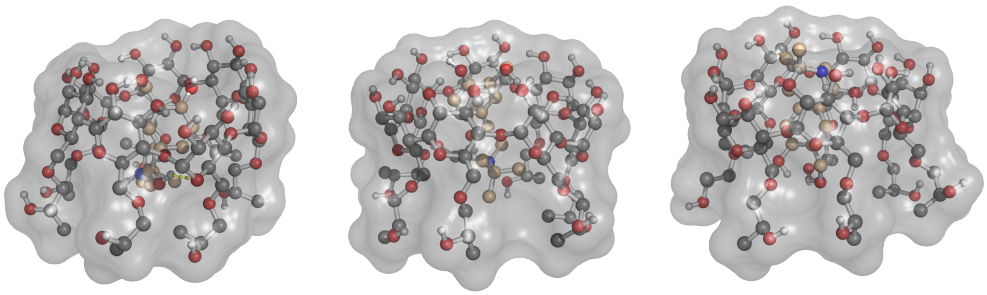

(a) binding mode 1 **(b)** binding mode 2 **(c)** binding mode 3

Figure 3.34: Binding modes between Hp-β-CyD and SAL after molecular docking calculations.

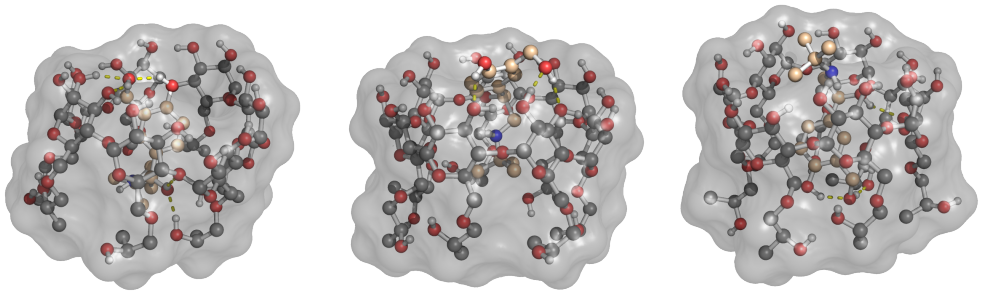

(a) binding mode 1 **(b)** binding mode 2 **(c)** binding mode 3

Figure 3.35: Optimized structures of binding mode 1, 2 and 3 between Hp-β-CyD and SAL after QM calculations.

In conclusion, with the addition of the 2-hydroxypropyl groups to the β-CyD, we have an increase in the hydrophobicity of the cavity while still also increasing the possibility to create hydrogen bonds with the hydroxypropyl group. This change allowed a higher level of insertion of the corticosteriod guests, probably due to a better accommodation inside the cavity.

3.2.1.5 γ-cyclodextrin

The last host studied was γ-CyD and we identified two binding modes with the BDP drug. In both adducts the corticosteroid group is inside the cavity, while in the first one the carbonyl end group is near the narrow side of the host (**Figure 3.36a**), in the second one their relative position is inverted (**Figure 3.36b**). The QM optimizations confirmed these binding modes as energy minima.

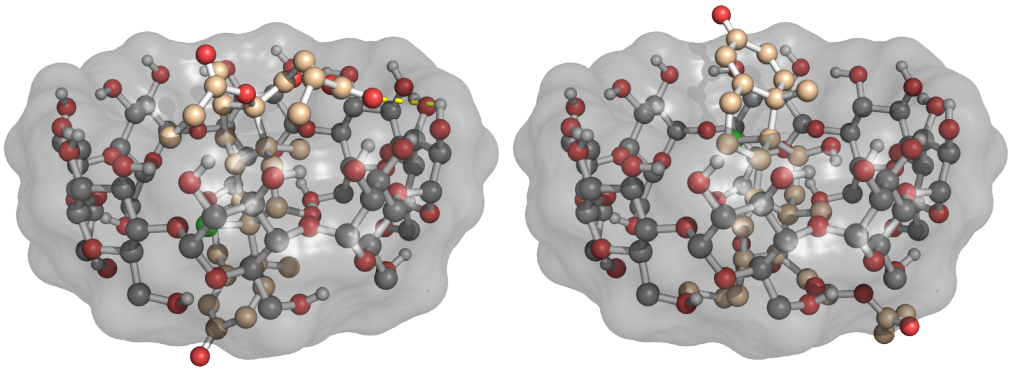

(a) binding mode 1 **(b)** binding mode 2

Figure 3.36: Binding modes between γ-CyD and BDP after molecular docking calculations.

The BUD drug also showed two binding modes with γ-CyD (**Figure 3.37**). Like previously, we also have two binding modes where the drug is in opposite configuration. In **Figure 3.37a** we have binding mode 1 with the carbonyl end located in the narrow side of γ-CyD, the corticosteroid group inside the cavity, and the other groups in the wider side. In binding mode 2, the guest structure is upside down, the corticosteroid group remains inside the cavity but the carbonyl end and the other groups of the molecule are in inverted positions (**Figure 3.37b**).

After the QM geometry optimization, in binding mode 1, we see a rear-

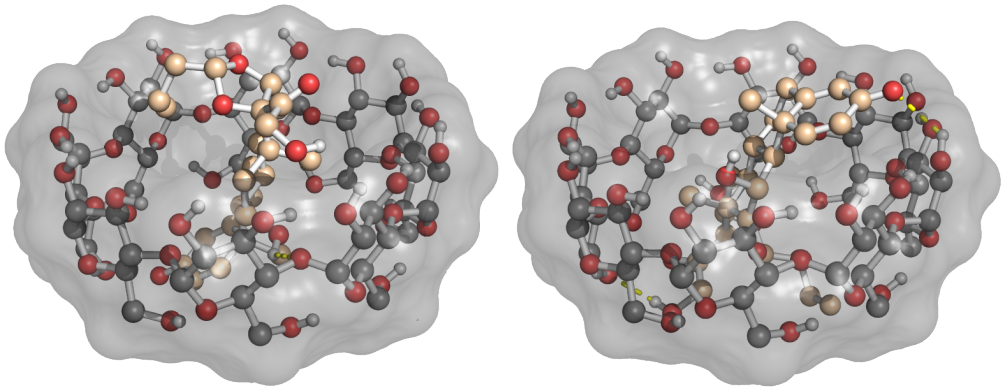

(a) binding mode 1 **(b)** binding mode 2

Figure 3.37: Binding modes between γ-CyD and BUD after molecular docking calculations.

rangement of the groups in the wider side of the host, allowing an hydroxyl group to hydrogen bonding in this region and another one, in the corticosteroid group, to approach the narrow side (**Figure 3.38a**). In binding mode 2, we have a slight displacement of the guest from the cavity to the wider side of the host, which was promoted by the formation of hydrogen bonds between the carbonyl end and hydroxyl groups of the corticosteroid on this side, and another one, on the narrow side, between two hydroxyl groups, one of the drug and one of the γ-CyD (**Figure 3.38b**).

We also identified two binding modes between CIC and γ-CyD. We observed a similar behavior: one geometry with the carbonyl end of the corticosteroid group in the narrow side of the γ-CyD, and the remaining groups in the wider side (**Figure 3.39a**); while in binding mode 2, these groups are in the opposite locations (**Figure 3.39b**). The QM calculations revealed a significant rearrangement in binding mode 2 (**Figure 3.40**). In this configuration, and similarly to what we have observed with previous drugs CIC is displaced outside the cavity to favor the formation of new hydrogen bonds with the host.

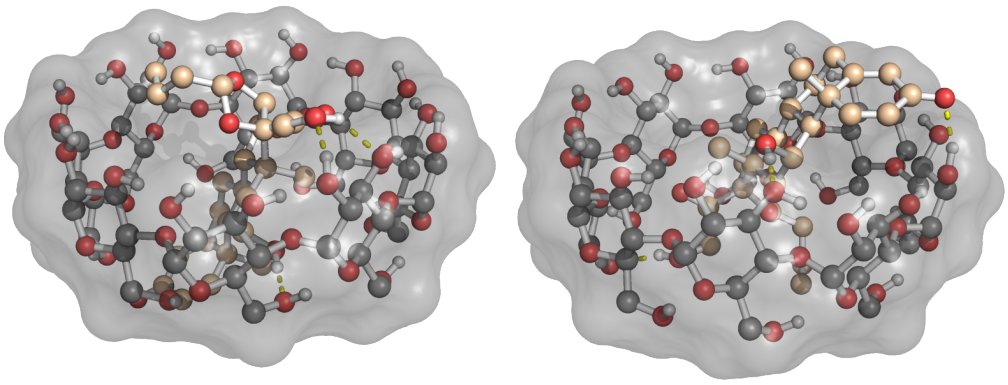

(a) binding mode 1 **(b)** binding mode 2

Figure 3.38: Optimized structures of binding mode 1 and 2 between γ-CyD and BUD after QM calculations.

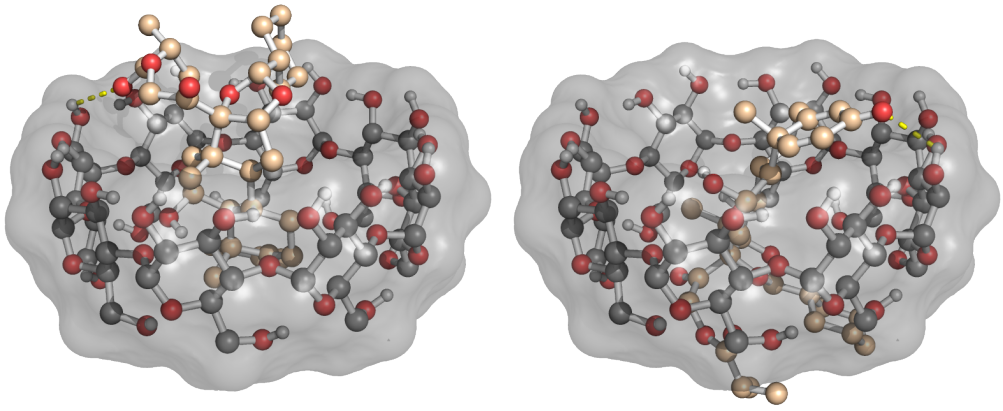

(a) binding mode 1 **(b)** binding mode 2

Figure 3.39: Binding modes between γ-CyD and CIC after molecular docking calculations.

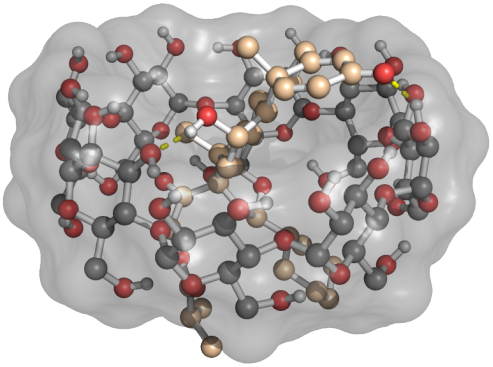

Figure 3.40: Optimized structure of binding mode 2 between γ-CyD and CIC after QM calculations.

We also identified two main binding modes between FP and γ-CyD (**Figure 3.41**), where the drug is in an inverted position between both adducts. In binding mode 1, the carbonyl end group is in the wider side of the host with the remaining groups in the narrow (**Figure 3.41a**). In binding mode 2 these groups are located in the wider side, with the carbonyl end in the narrow side (**Figure 3.41b**). The QM calculations confirmed these binding modes were very close to minima configurations.

Like what was observed for all drugs with γ-CyD, SAL also resulted in two binding modes. In both binding modes, we have the drug encapsulated in the host, with the only difference lying in the guest orientation. While in binding mode 1 the hydroxyl groups of the aromatic ring are turned to the wider side of the γ-CyD (**Figure 3.42a**), in binding mode 2 they are inverted and facing the narrow region (**Figure 3.42b**). The QM calculations showed a significant rearrangement of the guest's hydroxyl groups, specially in binding mode 1 (**Figure 3.43**). In binding mode 1, due to the high inclusion of the guest, we see an interaction between the secondary hydroxyl group in the aromatic ring of the guest and the oxygen atom that connects the subunits in the host. Also, in the narrow side, there is an interaction

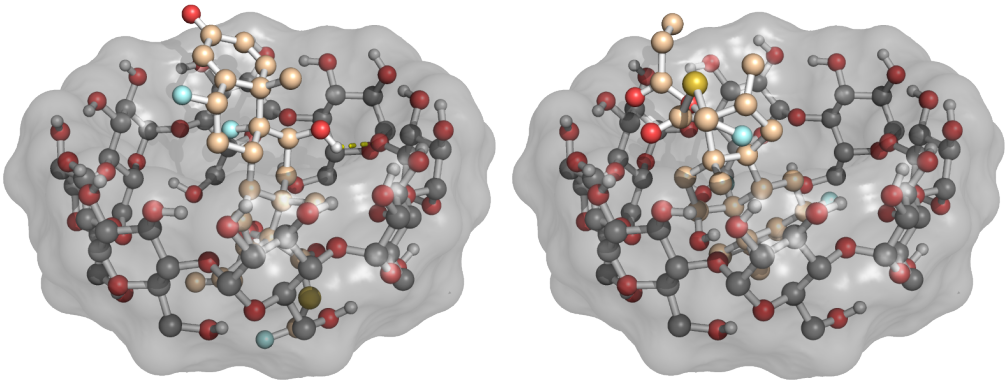

(a) binding mode 1 **(b)** binding mode 2

Figure 3.41: Binding modes between γ-CyD and FP after molecular docking calculations.

between the hydroxyl group of the host and the hydroxyl group of the linear group of the guest (**Figure 3.43a**). In binding mode 2, with an inverted conformation of the guest, the interaction with the oxygen atom is also present, but in this case it is established by the hydroxyl group of the linear group while the two hydroxyl groups of the aromatic ring are interacting with the primary hydroxyl groups in the narrow side of the γ-CyD (**Figure 3.43b**).

γ-CyD has an extremely wide cavity, which may be inconvenient to accommodate smaller guest molecules, like SAL, due to the free space that remains available in the hydrophobic region. With the largest corticosteroid molecules, γ-CyD is able to accommodate them, even though the final optimized structure suggest that there is no enough complementary as, quite often, the drug slides out of the cavity in order to establish hydrogen bonds with the host.

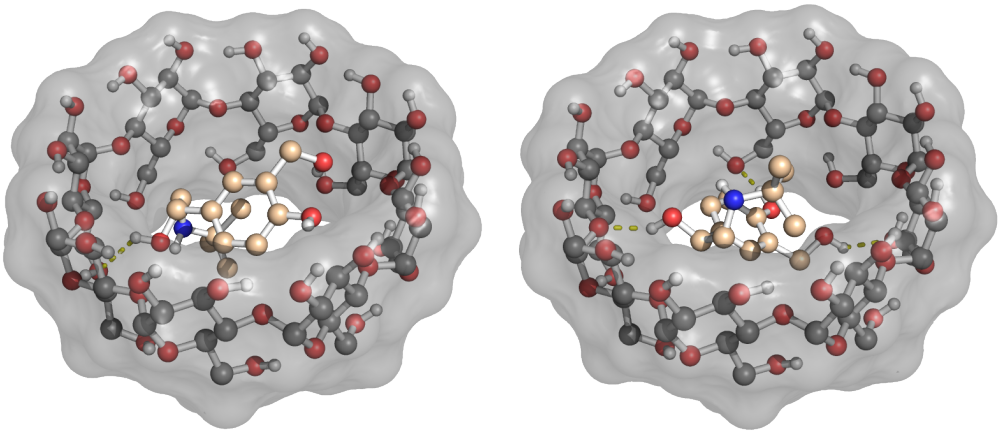

(a) binding mode 1 **(b)** binding mode 2

Figure 3.42: Binding modes between γ-CyD and SAL after molecular docking calculations.

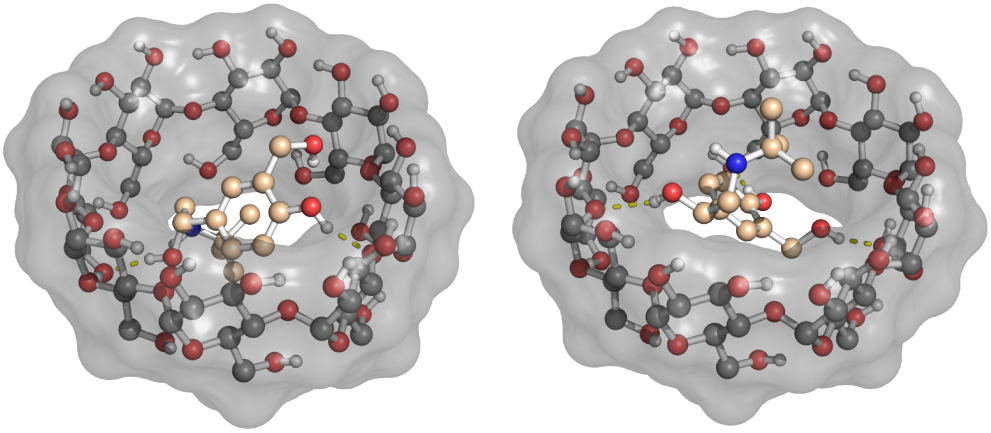

(a) binding mode 1 **(b)** binding mode 2

Figure 3.43: Optimized structures of binding 1 and 2 between γ-CyD and SAL after QM calculations.

3.2.2 Binding modes energies

In the next table are presented the electronic, enthalpic and Gibbs energies of binding (**Table 3.1**) for all adducts studied. Most of the electronic binding energies (ΔE) were already calculated except for two cases which are still running. The enthalpic (ΔH) and Gibbs (ΔG) binding energies require the calculation of the frequency values. However, in several cases, these calculations are very expensive computationally (they can run for several months), and are not completed at the time of this thesis submission. All calculations were obtained using **Equation 2.9** in **section 2.4**.

All ΔE binding energies calculated are negative, resulting in adducts more stable than the individual parts. A more detailed view shows that, BDP adducts are more stable with α-, Me- and Hp-β-CyD which is in excellent qualitative agreement with the experimental data [**16**] in **Table 1.2**. In fact, the highest stability constant measured for this drug (681.6 M^{-1}) was in an adduct with Hp-β-CyD and, from our calculations, the second binding mode presented the more negative electronic binding constant (-53.3 kcal·mol^{-1}). The BUD drug seems to form more stable adducts with γ- and Hp-β-CyDs, in this order (**Table 3.1**). This is also the preference observed in the available experimental data (**Table 1.2**) [**17**]. Our calculations also shows that CIC forms the most stable adducts with Hp-β-CyD. Even though, the stability constant of this adduct is significantly high (**Table 1.2**), the experimental data also showed that the best adduct is in fact Me-β-CyD. The fact that none of the binding modes with Me-β-CyD proved to be as stable as the one with Hp-β-CyD, tells us that the best adduct was not correctly sampled by the molecular docking procedure, or that there is a contribution (e.g. entropy) to the binding energy that is not visible in the electronic energies. Something similar happened with FP, where the experimental data shows a significantly more stable adduct with γ-CyD compared with Hp-β-CyD (**Table 1.2**). Our calculations show that indeed γ-CyD has a more negative electronic binding energy, however, the difference is very small (less than 2 kcal·mol^{-1}). The non-corticosteroid

SAL is interesting because, due to its smaller size, we have all calculations finished and this allow us to compare with the electronic, enthalpic and Gibbs binding energies of all binding modes.

In agreement with the experimental stability constant obtained by Marques [**21**], α- and γ-CyD are not good host molecules probably due to their too small or too large cavities, respectively. The lower binding energies for β- and Me-β-CyD are in excellent agreement with the higher K_s values measured experimentally [**21**]. Interestingly, our computational data indicate that SAL would have an even higher stability constant if Hp-β-CyD would be used as an host.

The study with SAL also allows us to compare the three types of binding energies (ΔE, ΔH and ΔG). It seems that the frequency correction needed to obtain both the enthalpic and Gibbs binding energies, does not invert the order of the preferred binding modes. This observation is very important to validate the qualitative analysis that we performed using the electronic binding energies. In fact, the ΔH binding energies are usually very similar to the ΔE ones. The most significant changes appear in the free Gibbs energy calculations which include an entropic correction and can have a major impact in the final values. As an example, we observed a very large entropic energy penalty for the adducts of SAL and γ-CyD, where the drug has too much conformational freedom in the host's cavity, and this resulted in positive free Gibbs energies.

The ΔG obtained between α-CyD and BDP for both binding modes is remarkably low. This adduct has already been identified experimentally to be very stable [**16**]. These authors proposed that α-CyD can stabilise both low molecule weight drugs or larger molecules exhibiting side groups that are able to insert in the host's cavity. BDP seems to fulfill all these criteria, resulting in a strong adduct with α-CyD.

Table 3.1: Electronic, enthalpic and Gibbs energies of binding (kcal·mol^{-1}) obtained for each adduct studied.

CyD	Drug	Binding mode	ΔE	ΔH	ΔG
α	BDP	1	-44.5	-42.7	-26.2
		2	-36.7	-35.2	-20.4
	BUD	1	-25.2	-23.9	-5.5
		2	-11.0	-10.0	5.3
	CIC	1	-31.3	**b**	
		2	-14.0	-12.4	6.9
	FP	1	-32.6	**b**	
		2	-26.5	-25.5	-10.4
		3	-20.2	**b**	
	SAL	1	-15.3	-13.7	3.0
		2	-18.6	-17.3	-2.4
β	BDP	1	-20.1		
		2	-21.0		
		3	-35.9		
	BUD	1	-13.1		
		2	-12.4		
		3	-26.7	**b**	
	CIC	1	-16.5		
		2	-27.8		
	FP	1	-29.1		
		2	-21.8		
		3	-19.6		
	SAL	1	-30.6	-28.9	-10.4
		2	-27.6	-26.5	-9.4

Me-β	BDP	1	-17.2	**b**	
		2	-48.9		
	BUD	1	**a**		
		2	-16.3		
		3	-15.9		
	CIC	1	-33.2		
		2	-23.6		
		3	-26.8		
	FP	1	-30.7		
		2	-15.7		
		3	-17.3		
		4	-31.6		
	SAL	1	-22.0	-20.7	-2.5
		2	-23.4	-21.9	-5.6
Hp-β	BDP	1	-32.4	**b**	
		2	-53.3		
		3	**a**		
	BUD	1	-22.5		
		2	-25.4		
		3	-27.9		
		4	-31.8		
	CIC	1	-39.9		
		2	-49.0		
	FP	1	-28.2		
		2	-18.5		
	SAL	1	-32.0	-25.4	-7.4
		2	-35.5	-33.8	-14.1
		3	-31.1	-29.4	-10.3
γ	BDP	1	-37.2	**b**	
		2	-34.0		
	BUD	1	-33.7		
		2	-32.9		
	CIC	1	-30.5		
		2	-36.6		
	FP	1	-29.6		
		2	-15.7		
	SAL	1	-9.6	-8.0	9.0
		2	-16.0	-14.8	3.4

a - Optimization calculations still running.

b - Frequency calculations still running.

Chapter 4

Concluding Remarks

The ability of CyDs to form inclusion complexes with guest molecules has two key factors, size complementary and specific interactions. The first one depends on the relative size of the CyD cavity compared to the guest molecule. The second factor concerns the driving forces allowing the guest to form stable adducts with the CyDs, taking in consideration that these hosts have some hydrophobic and other more hydrophilic regions and several hydroxyl groups that are able to act as both donor and acceptor of hydrogen bonds. Along these lines, we observed α-CyD, due to its smaller cavity space, is more appropriate to accommodate small molecules or even just side groups of larger compounds. γ-CyD has a quite large cavity and, while being able to accommodate all the drugs studied, if they are not large enough. It is not possible to maximize the number of stabilizing interactions and an energy penalty arises in such cases. The β-CyD seems to have the right number of subunits, giving the best close-fit for most guest molecules and allowing a better approximation to their wider and narrow side. The derivatizations of this CyD, like Me- and Hp-β-CyD, fine tuned the host properties by changing its hydrophobicity and the interaction patterns.

In overall, our computational approach was able to correctly predict qualitatively the best matches between the anti-asthmatic drugs and the CyDs.

We expect that the Gibbs free energies of binding, when finished, will corroborate what has been already observed. One example, is the adduct between SAL and Hp-β-CyD, which the stability has not been studied experimentally, but we expect it to be very strong.

This remarkable predictive ability shows that our computational method can be a powerful tool designing new and unexplored combinations of adducts.

Bibliography

[1] K. Mullane. The increasing challenge of discovering asthma drugs. *Biochem. Pharmacol.*, 82:586–599, 2011.

[2] D. R. Taylor, E. D. Bateman, L-P. Boulet, H. A. Boushey, W. W. Busse, T. B. Cassle, P. Chanez, P. L. Enright, P. G. Gibson, J. C. de Jongste, H. A. M. Kerstjens, S. C. Lazarus, M. L. Levy, P. M. O'Byrne, M. R. Partridge, I. D. Pavord, M. R. Sears, P. J. Sterk, S. W. Stoloff, S. J. Szefler, S. D. Sullivan, M. D. Thomas, S. E. Wenzel, and H. K. Reddel. A new perspective on concepts of asthma severity and control. *Eur. Resp. J.*, 32:545–554, 2008.

[3] Z. Diamant, J. D. Boot, and J. C. Virchow. Summing up 100 years of asthma. *Resp. Med.*, 101:377–388, 2007.

[4] S. P. Peters, G. Ferguson, Y. Deniz, and C. Reisner. Uncontrlolled asthma: A review of the prevalence, disease burden and options for treatment. *Resp. Med.*, 100:1139–1151, 2006.

[5] J. R. Murdoch and C. M. Lloyd. Chronic inflammation and asthma. *Mutat. Res-Fund. Mol. M.*, 690:24–39, 2010.

[6] E. D. Bateman, S. S. Hurd, P. J. Barnes, J. Bousquet, J. M. Drazen, M. FitzGerald, P. Gibson, K. Ohta, P. O'Byrne, S. E. Pedersen, E. Pizzichini, S. D. Sullivcan, S. E. Wenzel, and H.J. Zar. Global strategy for asthma management and prevention: Gina executive summary. *Eur. Resp. J.*, 31:143–178, 2008.

[7] K. A. Connors. The stability of cyclodextrin complexes in solution. *Chem. Rev.*, 97:1325–1357, 1997.

[8] S. Skowron. Cyclodextrin. http://en.wikipedia.org/wiki/Cyclodextrin#mediaviewer/File:Cyclodextrin.svg, accessed in August 2014.

[9] J. Szejtli. Introduction and general overview of cyclodextrin chemistry. *Chem. Rev.*, 98:1743–1753, 1998.

[10] E. M. Del Valle. Cyclodextrins and their uses: a review. *Process Biochem.*, 39:1033–1046, 2004.

[11] T. Loftsson and D. Duchêne. Cyclodextrins and their pharmaceutical applications. 329:1–11, 2007.

[12] Z. Li, M. Wang, and F. Wang. γ-cyclodextrins: a review on enzymatic production and apllications. *Appl. Microbiol. Biot.*, 77:245–255, 2007.

[13] J. Szejtli. Past, present and future of cyclodextrin research. *Pure Appl. Chem.*, 76:1825–1845, 2004.

[14] L. Liu and Q. Guo. The driving forces in the inclusion complexation of cyclodextrins. *J. Incl. Phenom. Macro.*, 42:1–14, 2002.

[15] K. Uekama, F. Hirayama, and T. Irie. Cyclodextrin drug carrier systems. *Chem. Rev.*, 98:2045–2076, 1998.

[16] B. Malaekeh-Nikouei, S. A. S. Tabassi, G. Gerayeli, M. A. Salmani, and A. Gholamzadeh. The effect of cyclodextrin mixtures on aqueous solubility of beclomethasone dipropionate. *J. Incl. Phenom. Macrocycl. Chem.*, 72:383–387, 2012.

[17] T. Kinnarinen, P. Jarho, and K. Jarvinen. Pulmonary deposition of budesonide/γ-cyclodextrin complex in vitro. *J. Control. Release*, 90:197–205, 2003.

[18] N. Arriagas and H. Cabral-Marques. Obtention and characterization of a ciclesonide: methyl-beta cyclodextrin complex. *J. Incl. Phenom. Macrocycl. Chem.*, 80:125–132, 2014.

[19] T. Oberski. Hydroxypropyl-beta-cyclodextrin/ciclesonide complexes for inhalation powders. Master's thesis, Faculty of Pharmacy of University of University of Ljubljana, Ljubljana, 2012.

[20] U. Leben. Fluticasone propionate/gamma-cyclodextrin complexes for pulmonary delivery. Master's thesis, Faculty of Pharmacy of University of University of Ljubljana, Ljubljana, 2012.

[21] H. M. Cabral Marques, J. Hadgraft, and I. W. Kellaway. Studies of cyclodextrin inclussion complexes. I. The salbutamol-cyclodextrin complex as studied by phase solubility and dsc. *Int. J. Pharm.*, 63:259–266, 1990.

[22] N. Zettili. *Quantum mechanics: concepts and applications.* John Wiley & Sons, UK, 2009.

[23] J. M. A. Henriques. Application of QM e MM methodologies to cytochorome c_3: charge parametrization of the heme group for classic force fields. Master's thesis, Faculdade de Ciências da Universidade de Lisboa, Lisboa, 2010.

[24] J. C. Slater. A simplification of the Hartree-Fock method. *Phys. Rev.*, 81:385–390, 1951.

[25] K. B. Lipkowitz. Applications of computational chemistry to the study of cyclodextrins. *Chem. Rev.*, 98:1829–1873, 1998.

[26] S. F. Sousa, P. A. Fernandes, and M. J. Ramos. Protein-ligand docking: current status and future challenges. *PSFB*, 65:15–26, 2006.

[27] D. B. Kitchen, H. Decornez, J. R. Furr, and J. Bajorath. Docking and scoring virtual screening for drug discovery: methods and applications. *Nat. Rev. Drug. Discovery*, 3:935–949, 2004.

[28] A. R. Leach. *Molecular modelling: principles and applications.* Pearson Education Limited, England, 2001.

[29] A. Szabo and N. S. Ostlund. *Modern quantum chemistry: Introduxtion to advanced electronic structure theory.* Dover Publicatioons, New York, 1996.

[30] P. Hohenberg and W. Kohn. Inhomogeneous electron gas. *Phys. Rev.*, 136, 1964.

[31] A. D. Becke. A new mixing of Hartree-Fock and local density functional theories. *J. Chem. Phys.*, 98:1372–1377, 1993.

[32] A. D. Becke. Density-functional exchange-energy approximation with correct asymptotic behavior. *Phys. Rev. A*, 38:3098–3100, 1988.

[33] C. Lee, W. Yang, and R. G. Parr. Development of the Colle-Salvetti correlation-energy formula into a functional of the electron density. *Phys. Rev. B*, 37:785–789, 1988.

[34] C. Adamo and V. Barone. Toward reliable density functional methods without adjustable parameters: The pbe0 model. *J. Chem. Phys.*, 110:6158–6170, 1999.

[35] J. P. Perdew, K. Burke, and M. Ernzerhof. Generalized gradient approximation made simple. *Phys. Rev. Lett.*, 77:3865–3868, 1996.

[36] J. P. Perdew, K. Burke, and M. Ernzerhof. Errata: Generalized gradient approximation made simple. *Phys. Rev. Lett.*, 78:1396, 1997.

[37] M. G. Teixeira, J. V. Assis, C. G. Soares, M. F. Venâncio, J. F. Lopes, C. S. Nascimento Jr, C. P A. Anconi, G. S. L. Carvalho, C. S. Lourenço, M. V. Almeida, S. A. Fernandes, and W. B. Almeida. Theoretical and experimental study of inclusion complexes formed by isoniazid and modified β-cyclodextrins: ^{1}H NMR structural determination and antibacterial activity evaluation. *J. Phys. Chem. B*, 118:81–93, 2014.

[38] W. J. Hehre, R. Ditchfield, and J. A. Pople. Self-consistent molecular orbital methods. xii. further exteinsions of Gaussian-type basis sets for use in molecular orbital studies of organic molecules. *J. Chem. Phys.*, 56:2257–2261, 1972.

[39] M. Chaplin. Cyclodextrin (jmol). http://www1.lsbu.ac.uk/water/cycloh.html, accessed in October 2013.

[40] The Metabolism Innovation Centre. Db00394.mol. http://www.drugbank.ca/structures/structures/small_molecule_drugs/DB00394.mol, accessed in October 2013.

[41] The Metabolism Innovation Centre. Db01222.mol. http://www.drugbank.ca/structures/structures/small_molecule_drugs/DB01222.mol, accessed in October 2013.

[42] The Metabolism Innovation Centre. Db01410.mol. http://www.drugbank.ca/structures/structures/small_molecule_drugs/DB01410.mol, accessed in October 2013.

[43] The Metabolism Innovation Centre. Db00588.mol. http://www.drugbank.ca/structures/structures/small_molecule_drugs/DB00588.mol, accessed in October 2013.

[44] The Metabolism Innovation Centre. Db01001.mol. http://www.drugbank.ca/structures/structures/small_molecule_drugs/DB01001.mol, accessed in October 2013.

[45] W L DeLano. The PyMOL molecular graphics system, 2002.

[46] M. handwell, D. E. Curtis, D. C. Lonie, and T. Vandermeersch. Avogadro: an advanced semantic chemical editor, visualization and analysis platform. *J. Cheminf.*, 4:1–17, 2012.

[47] T. A. Halgren. Merck molecular force field. I. Basis, form, scope, parametrization and performance of MMFF94. *J. Comput. Chem.*, 17:490–519, 1996.

[48] M. J. Frisch, G. W. Trucks, H. B. Schlegel, G. E. Scuseria, M. A. Robb, J. R. Cheeseman, G. Scalmani, V. Barone, B. Mennucci, G. A. Petersson, H. Nakatsuji, M. Caricato, X. Li, H. P. Hratchian, A. F. Izmaylov, J. Bloino, G. Zheng, J. L. Sonnenberg, M. Hada, M. Ehara, K. Toyota, R. Fukuda, J. Hasegawa, M. Ishida, T. Nakajima, Y. Honda, O. Kitao, H. Nakai, T. Vreven, J. A. Montgomery, Jr., J. E. Peralta, F. Ogliaro, M. Bearpark, J. J. Heyd, E. Brothers, K. N. Kudin, V. N. Staroverov, R. Kobayashi, J. Normand, K. Raghavachari, A. Rendell, J. C. Burant, S. S. Iyengar, J. Tomasi, M. Cossi, N. Rega, J. M. Millam, M. Klene, J. E. Knox, J. B. Cross, V. Bakken, C. Adamo, J. Jaramillo, R. Gomperts, R. E. Stratmann, O. Yazyev, A. J. Austin, R. Cammi, C. Pomelli, J. W. Ochterski, R. L. Martin, K. Morokuma, V. G. Zakrzewski, G. A. Voth, P. Salvador, J. J. Dannenberg, S. Dapprich, A. D. Daniels, Ö. Farkas, J. B. Foresman, J. V. Ortiz, J. Cioslowski, and D. J. Fox. Gaussian 09 Revision D.01. Gaussian Inc. Wallingford CT 2009.

[49] http://www.chemcraftprogg.com/index.html.

[50] D. S. Goodsell and A. J. Olson. Automated docking of substrates to proteins by simulated annealing. *Proteins: Struct. Funct. Genet.*, 8:195–202, 1990.

[51] A. R. Leach, B. K. Shoichet, and C. E. Peishoff. Prediction of protein-ligand interactions. docking and scoring: successes and gaps. *J. Med. Chem.*, 49, 2006.

[52] R. Wang, L. Lai, and S. Wang. Further development and validation of empirical scoring functions for structure-based binding affinity prediction. *J. Comp. Aid. Mol. Des.*, 16:11, 2002.

[53] O. Trott and A. J. Olson. Autodock vina: improving the speed and accuracy of docking with a new scoring function, efficient optimization, and multithreading. *J. Comput. Chem.*, 31:455–461, 2010.

[54] M. F. Sanner. Python: a programming language for software integration and development. *J. Mol. Graphics Mod.*, 17:57–61, 1999.

[55] S. Pronk, S. Páll, R. Schurlz, P. Larsson, P. Bjelkmar, R. Apostolov, M. R. Shirts, J. C. Smith, P. M. Kasson, D. van der Spoel, B. Hess, and E. Lindahl. GROMACS 4.5: a high-throughput and highly parallel open source molecular simulation toolkit. *Bioinformatics*, 2013.

[56] D. R. S. Vila-Viçosa. Reversibility of Prion Misfolding by Constant-pH Molecular Dynamics Simulations. Master's thesis, Faculdade de Ciências da Universidade de Lisboa, Lisboa, 2010.